Neri, F., Giolo, G., Potesta, M., Petrini, S., Doria, M., 2011. CD4 downregulation by the human immunodeficiency virus type 1 Nef protein is dispensable for optimal output and functionality of viral particles in primary T cells. J. Gen. Virol. 92, 141–150.

Noviello, C.M., Pond, S.L., Lewis, M.J., Richman, D.D., Pillai, S.K., Yang, O.O., Little, S.J., Smith, D.M., Guatelli, J.C., 2007. Maintenance of Nef-mediated modulation of major histocompatibility complex class I and CD4 after sexual transmission of human immunodeficiency virus type 1. J. Virol. 81, 4776–4786.

Premkumar, D.R., Ma, X.Z., Maitra, R.K., Chakrabarti, B.K., Salkowitz, J., Yen-Lieberman, B., Hirsch, M.S., Kestler, H.W., 1996. The nef gene from a long-term HIV type 1 nonprogressor. AIDS Res. Hum. Retroviruses 12, 337–345.

Schindler, M., Wurfl, S., Benaroch, P., Greenough, T.C., Daniels, R., Easterbrook, P., Brenner, M., Munch, J., Kirchhoff, F., 2003. Down-modulation of mature major histocompatibility complex class II and up-regulation of invariant chain cell surface expression are well-conserved functions of human and simian immunodeficiency virus nef alleles. J. Virol. 77, 10548–10556.

Schwartz, O., Marechal, V., Le Gall, S., Lemonnier, F., Heard, J.M., 1996. Endocytosis of major histocompatibility complex class I molecules is induced by the HIV-1 Nef protein. Nat. Med. 2, 338–342.

Stoddart, C.A., Geleziunas, R., Ferrell, S., Linquist-Stepps, V., Moreno, M.E., Bare, C., Xu, W., Yonemoto, W., Bresnahan, P.A., McCune, J.M., Greene, W.C., 2003. Human immunodeficiency virus type 1 Nef-mediated downregulation of CD4 correlates with Nef enhancement of viral pathogenesis. J. Virol. 77, 2124–2133.

Storey, J.D., Tibshirani, R., 2003. Statistical significance for genomewide studies. Proc. Nat. Acad. Sci. U.S.A. 100, 9440–9445.

Stumptner-Cuvelette, P., Morchoisne, S., Dugast, M., Le Gall, S., Raposo, G., Schwartz, O., Benaroch, P., 2001. HIV-1 Nef impairs MHC class II antigen presentation and surface expression. Proc. Nat. Acad. Sci. 98, 12144–12149.

Suzu, S., Harada, H., Matsumoto, T., Okada, S., 2005. HIV-1 Nef interferes with M-CSF receptor signaling through Hck activation and inhibits M-CSF bioactivities. Blood 105, 3230–3237.

Tobiume, M., Takahoko, M., Yamada, T., Tatsumi, M., Iwamoto, A., Matsuda, M., 2002. Inefficient enhancement of viral infectivity and CD4 downregulation by human immunodeficiency virus type 1 Nef from Japanese long-term nonprogressors. J. Virol. 76, 5959–5965.

Toussaint, H., Gobert, F.X., Schindler, M., Banning, C., Kozik, P., Jouve, M., Kirchhoff, F., Benaroch, P., 2008. Human immunodeficiency virus type 1 nef expression prevents AP-2-mediated internalization of the major histocompatibility complex class II-associated invariant chain. J. Virol. 82, 8373–8382.

Ueno, T., Motozono, C., Dohki, S., Mwimanzi, P., Rauch, S., Fackler, O.T., Oka, S., Takiguchi, M., 2008. CTL-mediated selective pressure influences dynamic evolution and pathogenic functions of HIV-1 Nef. J. Immunol. 180, 1107–1116.

Wei, X., Decker, J.M., Liu, H., Zhang, Z., Arani, R.B., Kilby, J.M., Saag, M.S., Wu, X., Shaw, G.M., Kappes, J.C., 2002. Emergence of resistant human immunodeficiency virus type 1 in patients receiving fusion inhibitor (T-20) monotherapy. Antimicrob. Agents Chemother. 46, 1896–1905.

Zhou, C., Lu, L., Tan, S., Jiang, S., Chen, Y.H., 2011. HIV-1 glycoprotein 41 ectodomain induces activation of the CD74 protein-mediated extracellular signal-regulated kinase/mitogen-activated protein kinase pathway to enhance viral infection. J. Biol. Chem. 286, 44869–44877.

Zuo, J., Suen, J., Wong, A., Lewis, M., Ayub, A., Belzer, M., Church, J., Yang, O.O., Krogstad, P., 2012. Functional analysis of HIV type 1 Nef gene variants from adolescent and adult survivors of perinatal infection. AIDS Res. Hum. Retroviruses 28, 486–492.

CD8+ T Cell Cross-Reactivity Profiles and HIV-1 Immune Escape towards an HLA-B35-Restricted Immunodominant Nef Epitope

Chihiro Motozono[1,2], John J. Miles[1,3,4], Zafrul Hasan[2], Hiroyuki Gatanaga[2,5], Stanley C. Meribe[2], David A. Price[1], Shinichi Oka[2,5], Andrew K. Sewell[1*©], Takamasa Ueno[2*©]

1 Institute of Infection and Immunity, Cardiff University School of Medicine, Heath Park, Cardiff, United Kingdom, 2 Center for AIDS Research, Kumamoto University, Kumamoto, Japan, 3 Australian Centre for Vaccine Development, Human Immunity Laboratory, Queensland Institute of Medical Research, Brisbane, Australia, 4 School of Medicine, The University of Queensland, Brisbane, Australia, 5 AIDS Clinical Center, National Center for Global Health and Medicine, Tokyo, Japan

Abstract

Antigen cross-reactivity is an inbuilt feature of the T cell compartment. However, little is known about the flexibility of T cell recognition in the context of genetically variable pathogens such as HIV-1. In this study, we used a combinatorial library containing 24 billion octamer peptides to characterize the cross-reactivity profiles of CD8+ T cells specific for the immunodominant HIV-1 subtype B Nef epitope VY8 (VPLRPMTY) presented by HLA-B*35:01. In conjunction, we examined naturally occurring antigenic variations within the VY8 epitope. Sequence analysis of plasma viral RNA isolated from 336 HIV-1-infected individuals revealed variability at position (P) 3 and P8 of VY8; Phe at P8, but not Val at P3, was identified as an HLA-B*35:01-associated polymorphism. VY8-specific T cells generated from several different HIV-1-infected patients showed unique and clonotype-dependent cross-reactivity footprints. Nonetheless, all T cells recognized both the index Leu and mutant Val at P3 equally well. In contrast, competitive titration assays revealed that the Tyr to Phe substitution at P8 reduced T cell recognition by 50–130 fold despite intact peptide binding to HLA-B*35:01. These findings explain the preferential selection of Phe at the C-terminus of VY8 in HLA-B*35:01+ individuals and demonstrate that HIV-1 can exploit the limitations of T cell recognition in vivo.

Introduction

Hypervariable viruses such as HIV-1 can escape from human leukocyte antigen class I (HLA-I)-restricted CD8+ T cell responses by acquiring viral genomic mutations within or near immunogenic epitopes. Such immune escape pathways can be extremely reproducible and broadly predictable based on host HLA-I alleles at a population level [1,2]. Somewhat paradoxically, however, antigen cross-reactivity is an inbuilt feature of the T cell compartment [3,4]. Indeed, a single autoimmune T cell receptor (TCR) has recently been shown to recognize more than a million different peptides within a broad cross-reactivity profile encompassing unrelated amino acid substitutions [5]. Furthermore, several lines of evidence suggest that certain CD8+ T cell subsets with the capacity to cross-recognize naturally occurring viral variants are advantageous for viral control in vivo [6–11]. However, the true extent of HIV-1-specific T cell cross-reactivity remains elusive. In the present study, we characterized the cross-reactivity footprints of HIV-1-specific CD8+ T cells using combinatorial peptide library (CPL) scanning to cover all possible amino acid variations at each position of an octamer epitope.

Additionally, we analyzed antigenic variation within the targeted epitope region of HIV-1 subtype B. Our investigations focused on CD8+ T cell responses specific for the immunodominant HIV-1 Nef epitope VY8 (VPLRPMTY) presented by HLA-B*35:01 [12,13].

Materials and Methods

Ethics Statement

All study participants provided informed, written consent at the AIDS Clinical Center, National Center for Global Health and Medicine, Japan. The study was approved by the Institutional Review Board of Kumamoto University and National Center for Global Health and Medicine.

Sequence Analysis of Autologous HIV-1

Treatment-naïve individuals (n = 336) with chronic HIV-1 infection (>90% subtype B) attending the AIDS Clinical Center (International Medical Center of Japan) were enrolled for autologous HIV-1 sequence analysis. The median [IQR] plasma viral load was 95,000 [31,000–350,000] copies/ml; the median

– 497 –

Table 1. TCR β composition of CD8⁺ T cell lines.

Patient	β chain			
	V gene	J gene	CDR3 sequence	Frequency
Pt-100	BV2*01	BJ2-7*01	CASSGEGNYEQYF	1/31
			CASTTDRVYEQYF	1/31
	BV3-1*01	BJ2-5*01	CASSTSSVTETQYF	2/31
		BJ2-7*01	CASSQDIAGVHEQYF	1/31
	BV4-1*01	BJ2-1*01	CASSQTSGSYNEQFF	1/31
	BV6-1*01	BJ1-5*01	CASSEASGIYEQYF	1/31
		BJ2-7*01	CASSEASGIYEQYF	1/31
	BV10-1*01	BJ2-1*01	CASSAAGVEYNEQFF	1/31
	BV11-2*01	BJ1-1*01	CASSFDIVNTEAFF	1/31
		BJ2-1*01	CASSPDLVDNEQFF	4/31
		BJ2-5*01	CASSGAWTGGGETQYF	2/31
		BJ2-7*01	CASSLDLVSYEQYF	1/31
			CASSLGIGRAYEQYF	1/31
	BV12-3*01	BJ1-4*01	CASSLRFATNEKLFF	1/31
	BV27*01	BJ2-5*01	CASSFDTNQETQYF	1/31
		BJ2-7*01	CASSLDTNGYEQYF	1/31
			CASSFQLAGVHGQYF	1/31
			CASSPRLDDEQYF	2/31
			CASSLDTSGYEQYF	2/31
			CASSSDREDSHEQYF	2/31
	BV28*01	BJ2-2*01	CASSSTDRAIPNTGELFF	1/31
		BJ2-3*01	CASSLPGLDSTDTQYF	1/31
		BJ2-7*01	CASSEGQGRYEQYF	1/31
Pt-168	BV2*01	BJ2-7*01	CASSESLAGGPYEQYF	7/31
	BV3-1*01	BJ2-3*01	CASSQEGADTQYF	2/31
	BV3-1*02	BJ2-3*01	CASSQEGAGTQYF	1/31
	BV6-2*01	BJ1-1*01	CASSGGRTDENTEAFF	1/31
		BJ2-1*01	CASSYEREDSGNEQFF	1/31
	BV11-2*01	BJ2-7*01	CASSLDVAGSYEQYF	1/31
			CASSLDIVSYEQYF	1/31
	BV11-3*03	BJ2-3*01	CASSLVLGTGTDTQYF	1/31
	BV12-3*01	BJ2-3*01	CASSWDSISTDTQYF	1/31
		BJ2-7*01	CASSSDGYEQYF	3/31
	BV12-5*01	BJ2-2*01	CASGLAMVVSGELFF	1/31
	BV15*02	BJ2-1*01	CATSRDLVEDEQFF	2/31
	BV20-1*05	BJ2-2*01	CSARDPRTDRGNTGELFF	1/31
	BV24-1*01	BJ2-3*01	CATSVRDDLTGNGPDTQYF	2/31
	BV27*01	BJ2-3*01	CASSLDLRPDTQYF	1/31
	BV28*01	BJ2-5*01	CASSLLGEETRETQYF	4/31
	BV30*01	BJ2-5*01	CAWHTVRVQETQYF	1/31

doi:10.1371/journal.pone.0066152.t001

[IQR] CD4⁺ T cell count was 242 [64.5–367.5] cells/mm³. We determined autologous *nef* sequences from plasma viral RNA using a previously reported direct sequencing method [13].

Table 2. TCR β composition of CD8⁺ T cell clones.

Patient	Clone	β chain		
		V gene	J gene	CDR3 sequence
Pt-19	19-136	BV7-2*03	BJ2-1*01	CASSPTPQGDYEQFF
	19-139	BV11-2*01	BJ1-1*01	CASSLDLVSTEAFF
Pt-33	33-S1	BV4-2*01	BJ2-3*01	CASSQAADAAITDADTQYF
Pt-100	100-K51	BV27*01	BJ2-5*01	CASSFDTNQETQYF
	100-K105	BV11-2*01	BJ1-1*01	CASSFDIVNTEAFF
	100-K810	BV27*01	BJ2-7*01	CASSFQLAGVHGQYF

doi:10.1371/journal.pone.0066152.t002

Generation and Maintenance of CD8⁺ T cell Lines and Clones

The CD8⁺ T cell clones (19-136, 19-139 and 33-S1) were established previously [13]. Additional CD8⁺ T cell lines and clones were generated by VY8 peptide stimulation of peripheral blood mononuclear cells (PBMCs) isolated from HLA-B*35:01⁺ individuals with chronic HIV-1 infection (Pt-100 and Pt-168) with 10 nM of VY8 (VPLRPMTY) peptide. The Institutional Review Board of the National Center for Global Health and Medicine approved both taking samples and generating cell lines, and patients provided the written informed consent. All CD8⁺ T cell lines and clones were maintained in RPMI 1640 supplemented with 10% fetal calf serum, 10 IU recombinant human interleukin (IL)-2, antibiotics and L-glutamine.

Analysis of TCR-encoding Genes

TCR-encoding genes of CD8⁺ T cell lines and clones were obtained by using a SMART PCR cDNA synthesis kit (Clontech) and analyzed with reference to the ImMunoGeneTics database (http://imgt.cines.fr) as described previously [14].

T cell Sensitivity Assay

Secretion of cytokines and chemokines by virus-specific CD8⁺ T cells in response to specific antigen provides a useful tool for quantitative assessment of antigen recognition [15,16]. MIP-1β was used as a functional readout in this study since it is one of the most sensitive means to assess functional avidity of human CD8⁺ T cells as previously described [15–17]. Briefly, 3×10^4 T cells were mixed with 6×10^4 HLA-B*35:01-expressing C1R cells (C1R-B3501), either unpulsed or pulsed with cognate peptide across a range of concentrations. After overnight incubation at 37°C, the supernatant was harvested and assayed for MIP-1β content by ELISA as described previously [5,17]. The amount of MIP-1β released in the absence of the peptide was subtracted as background. It should be noted that the VY8 peptide titration experiments of T cell clones 136 and 139 exhibited comparable results when IFN-γ [13] and MIP-1β were used as readouts (data not shown).

Figure 1. Amino acid residues preferentially recognized by VY8-specific CD8⁺ T cells. Graphical representation showing relative preference for amino acid residues recognized by VY8-specific T cell lines and clones based on the CPL scan data shown in Figure S1. Responses >20% were included. A web-based application, WebLogo 3 (http://weblogo.threeplusone.com/), was used to generate the graphic. Colours represent physicochemical properties: polar (G, S, T, Y and C), green; neutral (Q and N), purple; basic (K, R and H), blue; acidic (D and E), red; hydrophobic (A, V, L, I, P, W, F and M), black. The index residues at each position are outlined in yellow. Residue size is proportional to T cell recognition preference.
doi:10.1371/journal.pone.0066152.g001

Octamer Combinatorial Peptide Library (CPL) Scan

The octamer CPL contained a total of 2.4×10^{10} different peptides (PepScan) divided into 160 sub-mixtures in positional scanning format as described previously [4,18]. Target C1R-B3501 cells (6×10^4 cells/well) were pre-incubated in the absence or presence of CPL sub-mixtures (100 µg/ml). Effector T cells (3 x 10^4 cells/well) were then added and incubated overnight at 37°C. Supernatant was collected and analyzed for MIP-1β content by ELISA as described previously [5,17]. Background-subtracted results were expressed as % response, normalized with respect to the VY8 index residue. A response >20% was considered positive.

Results and Discussion

Clonotypic Characterization of VY8-specific T cells

CD8⁺ T cell lines were established from two $HLA\text{-}B^*35{:}01^+$ individuals with chronic HIV-1 infection (Pt-100 and Pt-168).

Analysis of TCR β usage by these T cell lines revealed multiple clonotypes, with 23 and 17 distinct TCR β sequences for Pt-100 and Pt-168, respectively (Table 1). This observation is consistent with previous studies showing the oligoclonal nature of immuno-dominant HIV-1-specific CD8⁺ T cell populations [19,20]. The CD8⁺ T cell clones K51, K105 and K810 were generated from patient Pt-100 by limiting dilution of VY8-specific T cell lines. Monoclonality was confirmed by TCR β analysis and all three sequences were encompassed within the TCR repertoire of the parental T cell lines (Table 2). Additional CD8⁺ T cell clones (136, 139, and S1) previously established from two separate $HLA\text{-}B^*35{:}01^+$ HIV-1-infected individuals [12,13] showed distinct TCR β chain usage (Table 2) and were also used for cross-reactivity studies.

- 499 -

A

B

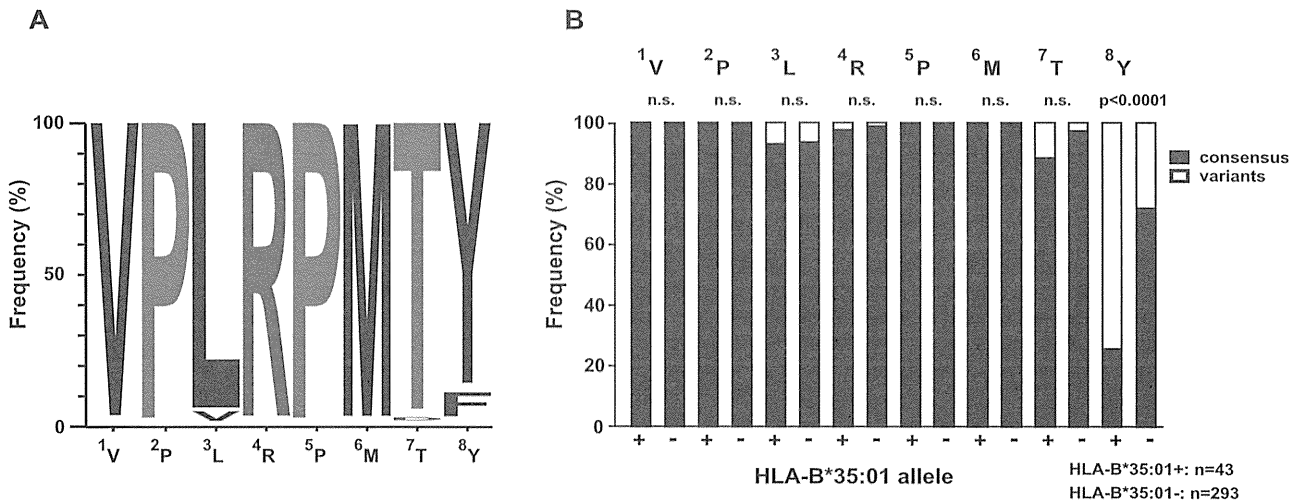HLA-B*35:01 allele

HLA-B*35:01+: n=43
HLA-B*35:01-: n=293

Figure 2. Naturally arising antigenic variations in the VY8 epitope. (A) Graphical representation showing the frequency of amino acid residues within the VY8 epitope in subtype B Nef sequences retrieved from the Los Alamos database (n = 1191). WebLogo 3 was used to generate the graphic. **(B)** The frequency of consensus (subtype B) and variant amino acid residues at each position of the VY8 epitope is shown for autologous plasma viral sequences derived from a total of 336 HIV-1-infected individuals, segregated according to HLA-B*35:01 status. Statistical analysis was performed using Fisher's exact test. n.s., not significant.
doi:10.1371/journal.pone.0066152.g002

Cross-reactivity Analysis of VY8-specific T cells

The cross-reactivity profiles of VY8-specific T cell lines and clones were analyzed using a CPL containing a total of 2.4×10^{10} different octamer peptides, which allowed qualitative mapping of preferred T cell recognition residues at each position along the peptide backbone [4,18]. Different VY8-specific T cell lines and clones preferentially recognized different amino acid residues across the octamer peptide backbone (Figure S1). We employed a graphical representation of these preferential recognition residues by the VY8-specific T cells (Figure 1). Despite these unique cross-reactivity patterns, all T cells tested recognized the index VY8 residues efficiently (Figure 1). This finding contrasts with previous observations using tumor-specific and autoreactive T cell clones [5,21–23], which typically prefer non-index amino acid residues. Across all clones, more stringent recognition was observed at

position 2 (P2) and P8 (Figure 1). This most likely reflects the anchor role of these positions in peptide binding to HLA-B*35:01 [12,24]. The VY8-specific T cell clones, K51, K105 and K810, showed inherently unique cross-reactivity footprints but less flexible cross-recognition compared to the parental T cell line (Figure 1), suggesting increased coverage of viral antigenic variation through polyclonal TCR cross-reactivity.

Naturally Occurring Antigenic variations within the VY8 Epitope

To investigate the correlation between T cell cross-reactivity and naturally occurring antigenic variation, we analyzed sequence polymorphisms within the VY8 epitope. Despite the remarkable variability of HIV-1 Nef, VY8 is highly conserved, most likely due to its location partially within a Src homology 3 binding motif that

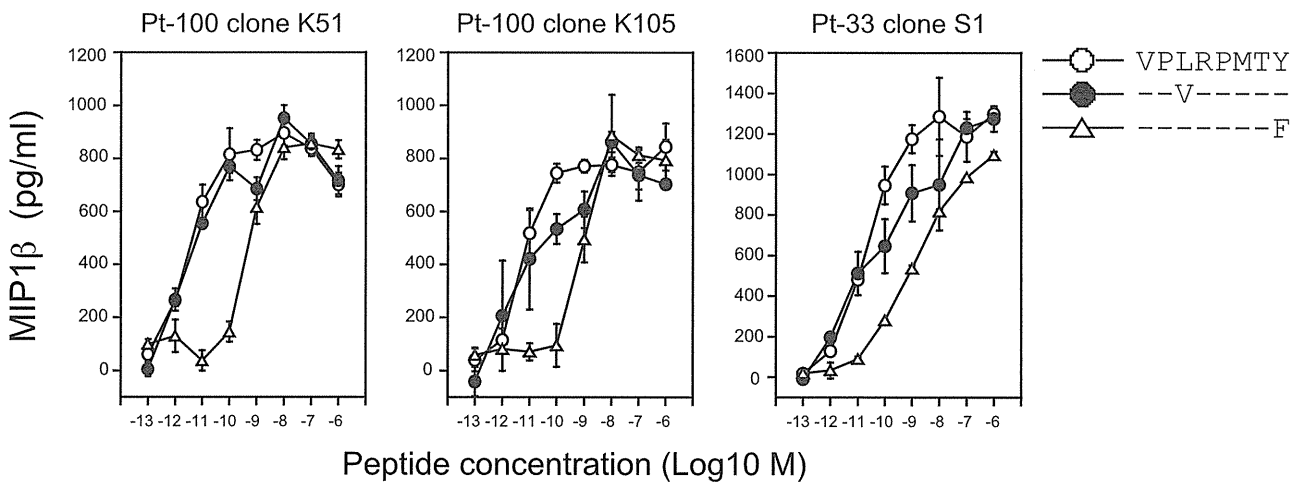**Figure 3. VY8-specific CD8+ T cell sensitivity towards peptide variants.** The sensitivity of T cell clones towards the VY8, VY8-3V and VY8-8F peptides was quantified by measuring the amount of MIP-1β secreted in response to antigen stimulation. Data are representative of duplicate assays and standard deviation from the mean of two replicates is shown.
doi:10.1371/journal.pone.0066152.g003

- 500 -

Table 3. Sensitivity of VY8-specific CD8⁺ T cells.

CD8⁺ T cells		EC₅₀ (M)		
		VY8	VY8-3V	VY8-8F
lines	Pt-100	5.9×10^{-12} (x 1)	nd	3.9×10^{-10} (x 66)
	Pt-168	4.0×10^{-12} (x 1)	nd	4.3×10^{-10} (x 105)
clones	33-S1	2.3×10^{-11} (x 1)	3.9×10^{-12} (x 0.17)	1.2×10^{-9} (x 52)
	100-K51	3.1×10^{-12} (x 1)	5.8×10^{-12} (x 1.8)	4.2×10^{-10} (x 135)
	100-K105	5.1×10^{-12} (x 1)	3.9×10^{-12} (x 0.76)	6.7×10^{-10} (x 131)

EC₅₀, determined by duplicate assays; nd, not done; in parenthesis, fold changes in sensitivity relative to index.
doi:10.1371/journal.pone.0066152.t003

is critical for several Nef functions [25], including HLA-I down-regulation [13,26]. Nevertheless, in the Los Alamos HIV Sequence database (http://www.hiv.lanl.gov/content/index), some variability within HIV-1 subtype B has been reported at P3 Leu and P8 Tyr of the VY8 epitope, with 2.4% and 8.2% of viral clones showing polymorphisms in these positions, respectively (Figure 2A). Given that approximately 40% of Nef sequence polymorphisms are associated with host HLA-I alleles [1], we examined these particular variants for HLA-I association. Our previous smaller study of 69 HIV-1-infected patients indicated that Phe at P8 might be associated with the $HLA\text{-}B^*35\text{:}01$ allele [13]. To confirm this association and examine polymorphisms at P3, we recruited a larger cohort comprising 336 treatment-naïve individuals with chronic HIV-1 infection and determined autologous *nef* sequences from plasma viral RNA. Although we found some variability at P3 (3%), there were no statistically significant amino acid differences at P1–P7 between individuals with or without $HLA\text{-}B^*35\text{:}01$ (Figure 2B). In fact, CPL scanning showed that, at P3, hydrophobic residues including both the index Leu and mutant Val were preferentially recognized by all VY8-specific T cells tested (Figure 1). Such flexible TCR recognition at P3 helps to explain why the Val mutant is not selected in $HLA\text{-}B^*35\text{:}01^+$ individuals. Conversely, we found a statistically significant difference in the frequency of polymorphisms at P8 between individuals with or without $HLA\text{-}B^*35\text{:}01$ (Figure 2B); indeed, the vast majority (74%) of $HLA\text{-}B^*35\text{:}01^+$ donors harboured viral sequences with Phe at P8. However, CPL scanning showed that Phe was a favoured amino acid residue recognized by T cell lines and some clones, such as K105 (Figure 1 and Figure S1). In these instances, CPL data alone do not simply explain the emergence of this viral mutation in $HLA\text{-}B^*35\text{:}01^+$ individuals.

VY8-specific T cell Sensitivity Towards Peptide Variants

To verify the effect of single mutations within the VY8 peptide on TCR sensitivity, we performed competitive titration assays across our panel of VY8-specific T cells (Figure 3). Consistent with the CPL scan data, all T cells tested recognized the VY8 and VY8-3V peptides comparably (<2 fold difference in EC₅₀ values; Table 3). In contrast, the EC₅₀ values for VY8-8F were >50 fold higher than index for all T cells tested (Table 3). These observations are consistent with previous reports showing that VY8-specific T cells could not recognize CD4⁺ T cells or macrophages infected with HIV-1 carrying this Nef variant at P8 [13,26].

Although P8 is an anchor residue for VY8, our previous HLA-I stabilization studies showed comparable binding activity between HLA-B*35:01 and either VY8 or VY8-8F [13]. The crystal

structure of the VY8/HLA-B*35:01 complex shows that P8 Tyr lies deep inside the F pocket of the HLA-I molecule [24]. Substitution at this position with the aromatic residue Phe may not induce substantial structural changes. Consequently, impaired T cell recognition of P8 Phe may be mediated by indirect conformational changes imposed by the peptide upon TCR binding [17]. In the context of HLA-A*02:01, however, a Tyr to Phe substitution at the secondary anchor P3 of an antigenic peptide (SLFNTVATL) leads to unexpectedly large conformational changes in the peptide backbone [27]. Accordingly, further structural studies are needed to elucidate the precise mechanism through which anchor residue substitution leads to impaired T cell recognition of the VY8 epitope.

Previous studies have shown that the double substitution of Arg-71 to Thr and Tyr-81 to Phe (P8 at VY8) [13], or Pro-75 to Ala (P2 at VY8) as a single mutation, impair Nef-mediated down-regulation of HLA-I and thereby increase the susceptibility of HIV-1-infected cells to killing by CD8⁺ T cells targeting other epitopes [26,28]. In contrast, the Tyr-81 to Phe (P8 at VY8) mutation alone exerts virtually no effect on Nef-mediated activities [13,26]. Collectively, these data suggest that the P8 Phe mutation does not compromise viral fitness.

Concluding Remarks

CD8⁺ T cell responses against the immunominant HIV-1 subtype B-derived Nef epitope VY8 presented by HLA-B*35:01 are highly polyclonal, broadly cross-reactive and capable of tolerating natural viral variation with one notable exception. Specifically, the observed Phe substitution at P8, which is neutral in terms of Nef-mediated function [13,26], was found to reduce CD8⁺ T cell recognition by >50 fold. The association of this mutation with $HLA\text{-}B^*35\text{:}01^+$ strongly suggests that evasion of VY8-specific CD8⁺ T cell activity confers a selection advantage *in vivo*. Thus, even CD8⁺ T cell responses with extensive cross-reactivity profiles can succumb to immune escape at a single position.

Supporting Information

Figure S1 CPL scanning of VY8-specific CD8⁺ T cells. The cross-reactivity profiles of T cell lines and clones specific for VY8 were tested by using 160 CPL sub-mixtures (100 µg/ml) comprising a total of 2.4×10^{10} different octamer peptides. In every peptide mixture, one position has a fixed amino acid residue and all other positions are degenerate, with the possibility of any one of 19 natural amino acids being incorporated in each individual position (cysteine is excluded). The amount of MIP-1β secreted in response to antigen was quantified by ELISA. Data are background-subtracted and the relative T cell response is shown as a ratio of MIP-1β production with respect to the index residue at each position. Responses >20% were considered positive and used to construct Figure 1. A representative set of duplicate assays is shown. Red bars depict residues corresponding to the VY8 index sequence.
(EPS)

Author Contributions

Conceived and designed the experiments: CM JJM AKS TU. Performed the experiments: CM JJM ZH SCM TU. Analyzed the data: CM JJM ZH

– 501 –

SCM DAP AKS TU. Contributed reagents/materials/analysis tools: HG SO. Wrote the paper: CM JJM DAP AKS TU.

References

1. Brumme ZL, John M, Carlson JM, Brumme CJ, Chan D, et al. (2009) HLA-associated immune escape pathways in HIV-1 subtype B Gag, Pol and Nef proteins. PLoS One 4: e6687.
2. Kawashima Y, Pfafferott K, Frater J, Matthews P, Payne R, et al. (2009) Adaptation of HIV-1 to human leukocyte antigen class I. Nature 458: 641–645.
3. Mason D (1998) A very high level of crossreactivity is an essential feature of the T-cell receptor. Immunol Today 19: 395–404.
4. Sewell AK (2012) Why must T cells be cross-reactive? Nat Rev Immunol 12: 669–677.
5. Wooldridge L, Ekeruche-Makinde J, van den Berg HA, Skowera A, Miles JJ, et al. (2012) A single autoimmune T cell receptor recognizes more than a million different peptides. J Biol Chem 287: 1168–1177.
6. Dong T, Stewart-Jones G, Chen N, Easterbrook P, Xu X, et al. (2004) HIV-specific cytotoxic T cells from long-term survivors select a unique T cell receptor. J Exp Med 200: 1547–1557.
7. Kosmrlj A, Read EL, Qi Y, Allen TM, Altfeld M, et al. (2010) Effects of thymic selection of the T-cell repertoire on HLA class I-associated control of HIV infection. Nature 465: 350–354.
8. Iglesias MC, Almeida JR, Fastenackels S, van Bockel DJ, Hashimoto M, et al. (2011) Escape from highly effective public CD8+ T-cell clonotypes by HIV. Blood 118: 2138–2149.
9. Chen H, Ndhlovu ZM, Liu D, Porter LC, Fang JW, et al. (2012) TCR clonotypes modulate the protective effect of HLA class I molecules in HIV-1 infection. Nat Immunol 13: 691–700.
10. Hoof I, Perez CL, Buggert M, Gustafsson RK, Nielsen M, et al. (2010) Interdisciplinary analysis of HIV-specific CD8+ T cell responses against variant epitopes reveals restricted TCR promiscuity. J Immunol 184: 5383–5391.
11. Ladell K, Hashimoto M, Iglesias MC, Wilmann PG, McLaren JE, et al. (2013) A Molecular Basis for the Control of Preimmune Escape Variants by HIV-Specific CD8(+) T Cells. Immunity 38: 425–436.
12. Motozono C, Yanaka S, Tsumoto K, Takiguchi M, Ueno T (2009) Impact of intrinsic cooperative thermodynamics of peptide-MHC complexes on antiviral activity of HIV-specific CTL. J Immunol 182: 5528–5536.
13. Ueno T, Motozono C, Dohki S, Mwimanzi P, Rauch S, et al. (2008) CTL-mediated selective pressure influences dynamic evolution and pathogenic functions of HIV-1 Nef. J Immunol 180: 1107–1116.
14. Ueno T, Tomiyama H, Takiguchi M (2002) Single T cell receptor-mediated recognition of an identical HIV-derived peptide presented by multiple HLA class I molecules. J Immunol 169: 4961–4969.
15. De Rosa SC, Lu FX, Yu J, Perfetto SP, Falloon J, et al. (2004) Vaccination in humans generates broad T cell cytokine responses. J Immunol 173: 5372–5380.
16. Betts MR, Nason MC, West SM, De Rosa SC, Migueles SA, et al. (2006) HIV nonprogressors preferentially maintain highly functional HIV-specific CD8+ T cells. Blood 107: 4781–4789.
17. Cole DK, Edwards ES, Wynn KK, Clement M, Miles JJ, et al. (2010) Modification of MHC anchor residues generates heteroclitic peptides that alter TCR binding and T cell recognition. J Immunol 185: 2600–2610.
18. Ekeruche-Makinde J, Miles JJ, van den Berg HA, Skowera A, Cole DK, et al. (2013) Peptide length determines the outcome of TCR/peptide-MHCI engagement. Blood 121: 1112–1123.
19. Douek DC, Betts MR, Brenchley JM, Hill BJ, Ambrozak DR, et al. (2002) A novel approach to the analysis of specificity, clonality, and frequency of HIV-specific T cell responses reveals a potential mechanism for control of viral escape. J Immunol 168: 3099–3104.
20. Meyer-Olson D, Brady KW, Bartman MT, O'Sullivan KM, Simons BC, et al. (2006) Fluctuations of functionally distinct CD8+ T-cell clonotypes demonstrate flexibility of the HIV-specific TCR repertoire. Blood 107: 2373–2383.
21. Wooldridge L, Laugel B, Ekeruche J, Clement M, van den Berg HA, et al. (2010) CD8 controls T cell cross-reactivity. J Immunol 185: 4625–4632.
22. Ekeruche-Makinde J, Clement M, Cole DK, Edwards ES, Ladell K, et al. (2012) T-cell receptor-optimized peptide skewing of the T-cell repertoire can enhance antigen targeting. J Biol Chem 287: 37269–37281.
23. Bulek AM, Cole DK, Skowera A, Dolton G, Gras S, et al. (2012) Structural basis for the killing of human beta cells by CD8(+) T cells in type 1 diabetes. Nat Immunol 13: 283–289.
24. Smith KJ, Reid SW, Stuart DI, McMichael AJ, Jones EY, et al. (1996) An altered position of the alpha 2 helix of MHC class I is revealed by the crystal structure of HLA-B*3501. Immunity 4: 203–213.
25. Saksela K, Cheng G, Baltimore D (1995) Proline-rich (PxxP) motifs in HIV-1 Nef bind to SH3 domains of a subset of Src kinases and are required for the enhanced growth of Nef+ viruses but not for down-regulation of CD4. EMBO J 14: 484–491.
26. Mwimanzi P, Hasan Z, Hassan R, Suzu S, Takiguchi M, et al. (2011) Effects of naturally-arising HIV Nef mutations on cytotoxic T lymphocyte recognition and Nef's functionality in primary macrophages. Retrovirology 8: 50.
27. Lee JK, Stewart-Jones G, Dong T, Harlos K, Di Gleria K, et al. (2004) T cell cross-reactivity and conformational changes during TCR engagement. J Exp Med 200: 1455–1466.
28. Yamada T, Kaji N, Odawara T, Chiba J, Iwamoto A, et al. (2003) Proline 78 is crucial for human immunodeficiency virus type 1 Nef to down-regulate class I human leukocyte antigen. J Virol 77: 1589–1594.

– 502 –

Natural Single-Nucleotide Polymorphisms in the 3' Region of the HIV-1 *pol* Gene Modulate Viral Replication Ability

Masako Nomaguchi,[a] Ariko Miyake,[a] Naoya Doi,[a] Sachi Fujiwara,[a] Yasuyuki Miyazaki,[a] Yasuko Tsunetsugu-Yokota,[b] Masaru Yokoyama,[c] Hironori Sato,[c] Takao Masuda,[d] Akio Adachi[a]

Department of Microbiology, Institute of Health Biosciences, The University of Tokushima Graduate School, Tokushima, Japan[a]; Department of Immunology, National Institute of Infectious Diseases, Tokyo, Japan[b]; Laboratory of Viral Genomics, Pathogen Genomics Center, National Institute of Infectious Diseases, Tokyo, Japan[c]; Department of Immunotherapeutics, Graduate School of Medicine and Dentistry, Tokyo Medical and Dental University, Tokyo, Japan[d]

ABSTRACT

We previously showed that prototype macaque-tropic human immunodeficiency virus type 1 (HIV-1) acquired nonsynonymous growth-enhancing mutations within a narrow genomic region during the adaptation process in macaque cells. These adaptive mutations were clustered in the 3' region of the *pol* gene, encoding a small portion of the C-terminal domain of integrase (IN). Mutations in HIV-1 IN have been reported to have pleiotropic effects on both the early and late phases in viral replication. *cis*-acting functions in the IN-coding sequence for viral gene expression have also been reported. We here demonstrated that the adaptive mutations promoted viral growth by increasing virion production with no positive effects on the early replication phase. Synonymous codon alterations in one of the adaptive mutations influenced virion production levels, which suggested nucleotide-dependent regulation. Indeed, when the single-nucleotide natural polymorphisms observed in the 3' regions of 196 HIV-1/simian immunodeficiency virus (SIVcpz) *pol* genes (nucleotides [nt] 4895 to 4929 for HIV-1 NL4-3) were introduced into macaque- and human-tropic HIV-1 clones, more than half exhibited altered replication potentials. Moreover, single-nucleotide mutations caused parallel increases or decreases in the expression levels of viral late proteins and viral replication potentials. We also showed that the overall expression profiles of viral mRNAs were markedly changed by single-nucleotide mutations. These results demonstrate that the 3' region of the HIV-1 *pol* gene (nt 4895 to 4929) can alter viral replication potential by modulating the expression pattern of viral mRNAs in a nucleotide-dependent manner.

IMPORTANCE

Viruses have the plasticity to adapt themselves under various constraints. HIV-1 can mutate and evolve in growth-restrictive cells by acquiring adaptive changes in its genome. We have previously identified some growth-enhancing mutations in a narrow region of the IN-coding sequence, in which a number of *cis*-acting elements are located. We now focus on the virological significance of this *pol* gene region and the mechanistic basis underlying its effects on viral replication. We have found several naturally occurring synonymous mutations within this region that alter viral replication potentials. The effects caused by these natural single-nucleotide polymorphisms are linked to the definite expression patterns of viral mRNAs. We show here that the nucleotide sequence of the *pol* gene (nucleotides 4895 to 4929 for HIV-1 NL4-3) plays an important role in HIV-1 replication by modulating viral gene expression.

The gene expression process of human immunodeficiency virus type 1 (HIV-1) (transcription, capping, polyadenylation, splicing, nuclear export, and translation) is highly coordinated and regulated by interactions between host/viral proteins and *cis*-acting elements located within the viral genome (1, 2). During this process, more than 40 mRNA species with nine viral genes are generated by alternative splicing (3, 4). These mRNA species are divided into three major groups: ~9-kb mRNAs (unspliced form) encoding Gag and Gag-Pol proteins, ~4-kb mRNAs (singly spliced form) encoding Vif, Vpr, Vpu, and Env proteins, and ~1.8-kb mRNAs (completely spliced form) encoding Tat, Rev, and Nef proteins. In the early phase of HIV-1 gene expression, ~1.8-kb mRNA species are transported to the cytoplasm and translated to synthesize Tat, Rev, and Nef proteins. Tat, along with some host factors, *trans*-activates HIV-1 transcription (5, 6). Rev facilitates the nuclear export of ~4-kb and ~9-kb HIV-1 mRNAs, and their encoded proteins are subsequently produced (7, 8). Alterations in the tightly regulated process of HIV-1 gene expression can affect viral replication (3, 4, 9–11).

HIV-1 integrase (IN) is generated from a Gag-Pol precursor and mediates integration, a hallmark of retroviruses. HIV-1 IN is involved not only in integration but also in reverse transcription, viral DNA nuclear import, and virion assembly/production (12–19). The deletion or C-terminal truncation of HIV-1 IN has been shown to reduce virion production in producer cells (20, 21). Although mutations in IN have negative effects on virion production, they also affect the early phase of viral replication (15, 22). Different amino acid substitutions at the same sites often have diverse effects on viral replication potential (13, 15, 23, 24). Furthermore, a number of splicing sites and *cis*-acting elements have been identified in the IN-coding sequence (3, 4, 25–30). There-

April 2014 Volume 88 Number 8
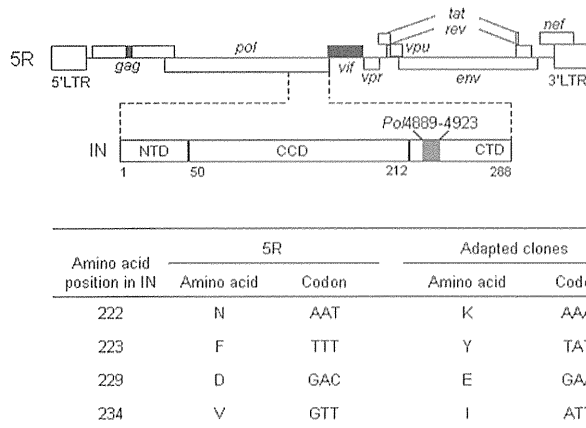Journal of Virology p. 4145–4160
jvi.asm.org 4145

FIG 1 Growth-enhancing mutations identified in the 3′ region of the *pol* gene. The genome structure of 5R (34) (GenBank accession no. AB266485) is schematically depicted. Black areas show the sequence derived from SIVmac239 (56) (GenBank accession no. M33262). The *pol* region encoding IN and the IN domain structure are indicated. The gray area represents a region in the *pol* gene (nt 4889 to 4923) designated *Pol*4889-4923, in which adaptive mutations are located. NTD, N-terminal domain; CCD, catalytic core domain; CTD, C-terminal domain. Details of the adaptive mutations found in the *Pol*4889-4923 region are shown at the bottom.

fore, mutations in the IN-coding sequence can change the nucleotide sequence important for viral replication as well as the protein-coding sequence associated with IN activity. The replication-defective mutant IN E246K represents a good example. It showed a processing defect in Gag, and its virion production level was markedly reduced (15). The E246K mutation, which is located within splicing site D2 and affects viral RNA splicing, was shown to result in the loss of viral infectivity (31). Thus, *cis*-acting functions in the IN-coding sequence must be considered to delineate its possible roles in viral replication.

In a previous virus adaptation study, we demonstrated that growth-enhanced viruses, which emerged following a long-term culture of cells infected with macaque-tropic HIV-1 NL-DT5R (5R) or NL-DT562 (562), frequently and reproducibly acquired mutations in the 3′ region of the *pol* gene (nucleotides [nt] 4889 to 4923 for 5R [Fig. 1] and nt 4895 to 4929 for the standard HIV-1 NL4-3), which encodes a small portion of the IN C-terminal domain (CTD) (32). Four adaptive mutations (N222K, F223Y, D229E, and V234I) in the region were identified in our repeated virus adaptation experiments and were responsible for viral growth enhancements (32). In this study, we aimed to elucidate how mutations in the 3′ region of the *pol* gene promoted viral replication and what the virological significance of this region was. The four mutations mentioned above were found to augment virus replication potential by increasing infectious virion production without any effects on the early replication phase. The CTD has been reported to be the least conserved sequence of the three domains in IN (15, 17, 19), with the 234th amino acid in IN being polymorphic (33). Codon alterations in V234I from ATT to ATC and ATA influenced virion production, which indicated regulation by a single-nucleotide change. An investigation of the sequences in the 3′ region of the *pol* gene in 196 HIV-1/simian immunodeficiency virus (SIVcpz) genomes (HIV sequence compendium 2011, Los Alamos National Laboratory, NM, USA) revealed that natural variants carried ATT or ATC at amino acid

position 234. Based on these findings, single-nucleotide natural variations in the 3′ region of the *pol* gene (nt 4895 to 4929 for NL4-3) were introduced into macaque- and human-tropic HIV-1 clones. We identified several natural variations that alter virion production/replication efficiency. The observed effects of single-nucleotide variations were attributed to an increase or decrease in the expression levels of viral late proteins (Gag, Gag-Pol, Vpu, and Env), whereas early proteins (Nef and Rev) were invariably expressed. Moreover, single-nucleotide variations caused changes in the viral mRNA expression pattern. Taken together, our results showed that the nucleotide sequence of the 3′ region of the HIV-1 *pol* gene (nt 4895 to 4929 for NL4-3) play an important role in viral replication by modulating viral gene expression.

MATERIALS AND METHODS

Plasmid DNAs. The proviral clones pNL-DT5R (34) and pNL4-3 (35) were used as parental clones in the present study. Proviral clones carrying each mutation in the 3′ region of the *pol* gene were constructed with the QuikChange site-directed mutagenesis kit (Agilent Technologies Inc., Santa Clara, CA). Proviral *env*-deficient clones were constructed by deleting the NdeI (nt 6584)-NheI (nt 7435) fragment of pNL-DT5R. Reporter clones were constructed by introducing the luciferase gene into the *nef* gene of *env*-deficient proviral clones as described previously (36). A long terminal repeat (LTR)-driven luciferase reporter clone (5RLTR-Luc) was constructed by replacing the AatII (5′end of the proviral genome)-NcoI (5′end of the luciferase gene in the *nef* gene) fragment of the pNL-DT5R luciferase reporter clone with the LTR region (nt 1 to 789) of pNL-DT5R. A proviral *gag/gag-pol* frameshift clone (gtg-Spe) was constructed by cutting the V234gtg clone with SpeI (nt 1501) within the *gag* capsid and inserting four nucleotides with T4 DNA polymerase.

Cells. Human kidney 293T cells were cultured in minimal essential medium (MEM) supplemented with 10% heat-inactivated fetal bovine serum (hiFBS). Human lymphocyte M8166 cells were cultured in RPMI 1640 supplemented with 10% hiFBS. Human lymphocyte MT4/CCR5 cells (MT4 cells stably expressing CCR5) were maintained in RPMI 1640 containing 10% hiFBS and 200 μg/ml of hygromycin B (Sigma-Aldrich Co., St. Louis, MO).

Analysis of virus growth kinetics. Virus stocks were prepared from 293T cells transfected with proviral clones as previously described (34, 35). Virion-associated reverse transcriptase (RT) activity was measured as previously described (37). M8166 and MT4/CCR5 cells (10^5) were infected with equal amounts of NL-DT5R and its derivative viruses (35 RT units and 5×10^5 RT units for M8166 and MT4/CCR5 cells, respectively), as previously described (38, 39). Equal amounts (10^5 RT units) of HIV-1 NL4-3 and its derivative viruses were inoculated into MT4/CCR5 cells (10^5). Virus replication was monitored by RT activity released into the culture supernatants.

Analysis of single-cycle viral infectivity. Vesicular stomatitis virus G protein (VSV-G)-pseudotyped viruses were prepared from 293T cells cotransfected with an *env*-deficient luciferase reporter clone and pCMV-G (40) at a molar ratio of 1:1. Virus amounts on day 2 posttransfection were measured with an HIV-1 p24 antigen enzyme-linked immunosorbent assay (ELISA) kit (ZeptoMetrix Corporation, Buffalo, NY). M8166 cells (10^5) were infected with equal amounts of pseudotyped viruses (30 pg of p24), and cells were lysed on day 1 postinfection for luciferase assays (Promega Corporation, Madison, WI).

Analysis of viral cDNA synthesis. DNase I-treated pseudoviruses (150 pg of p24) were inoculated into M8166 cells (5×10^5), and total DNA was extracted on day 1 postinfection using the DNeasy blood and tissue kit (Qiagen GmbH, Hilden, Germany). Quantitative analyses of viral cDNA products using real-time quantitative PCR (ABI7500; Life Technologies Corporation, Carlsbad, CA) were performed as previously described (14).

Analysis of virion production. M8166 cells (10^6) were cotransfected with equal amounts of *env*-deficient proviral clones (1 μg) and the pGL3

Amino acid position in IN	5R		Adapted clones	
	Amino acid	Codon	Amino acid	Codon
222	N	AAT	K	AAA
223	F	TTT	Y	TAT
229	D	GAC	E	GAA
234	V	GTT	I	ATT

– 504 –

luciferase reporter vector (Promega Corporation) (1 μg) using the Amaxa human T cell Nucleofector kit (Lonza Ltd., Basel, Switzerland) with Nucleofector II (Lonza Ltd.). Culture supernatants were collected on day 2 posttransfection, and virion production was measured using the HIV-1 p24 antigen ELISA kit (ZeptoMetrix Corporation). Cell lysates were prepared with 1× CCLR buffer (Promega Corporation) and subjected to luciferase assays (Promega Corporation). The luciferase activity in cell lysates was used to normalize the transfection efficiency.

Analysis of viral protein expression. 293T cells for Western blot analysis were transfected with equal amounts of proviral clones by using Lipofectamine 2000 (Life Technologies Corporation) in the absence or presence of 2 μM saquinavir (SQV) (Sigma-Aldrich Co.). On day 1 posttransfection, cells were lysed in 1× TNE buffer (10 mM Tris-HCl [pH 8.0], 1% Nonidet P-40, 150 mM NaCl, 1 mM EDTA [pH 8.0], and 1% protease inhibitor cocktail [Sigma-Aldrich Co.]). The total protein amounts in the cell lysates were measured with the DC protein assay (Bio-Rad Laboratories Inc., Hercules, CA), and equal amounts were loaded onto Mini-Protean TGX gels (Bio-Rad Laboratories Inc.) for electrophoresis (0.5 μg for the anti-gp160 antibody, 1 μg for the anti-Vpu antibody, 2 μg for the anti-p24, anti-Nef, or anti-β-actin antibody, 5 μg for the anti-Rev antibody, and 20 μg for the anti-RT antibody). Following blotting onto Immobilon-P transfer membranes (Merck KGaA, Darmstadt, Germany), the membranes were treated with the anti-β-actin clone AC-15 (Sigma-Aldrich Co.), anti-HIV-1 p24 (183-H12-5C) (catalog number 3537; NIH Research and References Reagent Program), anti-HIV-1 RT (MP Biomedicals, Santa Ana, CA), HIV-1 NL4-3 Vpu antiserum (catalog number 969; NIH Research and References Reagent Program), anti-HIV-1 gp160 (ADP409; Immuno Ltd./the MRC AIDS Directed Programme Reagent Project), anti-Rev (ab25871; Abcam PLC, Cambridge, England), or anti-HIV-1 Nef (Advanced Biotechnologies Inc., Columbia, MD) antibody and visualized with the Amersham ECL Plus Western blotting detection system (GE Healthcare UK Ltd., Buckinghamshire, England). A GS-800 calibrated densitometer and Quantity One software (Bio-Rad Laboratories Inc.) were used to quantify signal intensities. To monitor the expression levels of viral proteins, 293T cells were transfected with proviral clones by using Lipofectamine 2000 (Life Technologies Corporation), and on day 2 posttransfection, samples were prepared as described above. The amounts of cell-associated Gag-p24 and Pol-RT were measured using the HIV-1 p24 antigen ELISA kit (ZeptoMetrix Corporation) and RT capture ELISA kit (ImmunoDX, LLC, Woburn, MA), respectively. To monitor Tat activity, 293T cells were cotransfected with proviral clones (0.2 μg) and the 5RLTR-Luc clone (0.05 μg) by using Lipofectamine 2000 (Life Technologies Corporation). Cells were lysed with 1× CCLR buffer (Promega Corporation) on day 1 posttransfection for luciferase assays (Promega Corporation). 293T cells for the interference experiments were transfected with an appropriate amount of proviral clones (5R and its derivatives) by using Lipofectamine 2000 (Life Technologies Corporation). Cells were lysed with 1× TNE buffer on day 1 posttransfection, and the amount of Gag-p24 in cell lysates was measured using the HIV-1 p24 antigen ELISA kit (ZeptoMetrix Corporation).

Northern blot analysis. 293T cells were transfected with equal amounts of proviral clones by using Lipofectamine 2000 (Life Technologies Corporation), and total RNA was extracted at 10 to 20 h posttransfection using the RNeasy Plus Minikit (Qiagen GmbH). Poly(A)$^+$ RNA was isolated with the Oligotex-dT30 Super mRNA purification kit (TaKaRa Bio Inc., Otsu, Japan) and then treated with DNase I (TaKaRa Bio Inc.). Equal amounts of RNA samples were loaded on a glyoxal denatured 1% agarose gel prepared with NorthernMax-Gly 10× Gel Prep/running buffer (Life Technologies Corporation), electrophoresed, and blotted onto a positively charged nylon membrane (Roche Diagnostics GmbH, Mannheim, Germany). The digoxigenin (DIG)-labeled universal probe (U probe) to detect all HIV-1 mRNA species was prepared by using a PCR DIG probe synthesis kit (Roche Diagnostics GmbH.) with pNL4-3 as a template and primers 5'-GAGGATTGTGGAACTTCTGG-3' and 5'-CT TTGGGAGTGAATTAGCCC-3'. The DIG-labeled Rev-responsive ele-

ment (RRE) probe, vif probe, and vpr probe were synthesized using templates and primer pairs as follows: RRE probe, pNL4-3, forward primer 5'-CCATTAGGAGTAGCACCCAC-3', and reverse primer 5'-GTTCCA GAGATTTATTACTCC-3'; vif probe, pNL-DT5R, forward primer 5'-AT GGAGGAGGAAAAGAGGTGG-3', and reverse primer 5'-CTGCATAA GTACTGAGCCAC-3'; and vpr probe, pNL4-3, forward primer 5'-ATG GAACAAGCCCCAGAAG-3', and reverse primer 5'-GCAGAATTCTTA TTATGGCTTCC-3'. The membrane was hybridized with the DIG-labeled probe in DIG Easy Hyb (Roche Diagnostics GmbH), and visualized with the DIG High Prime DNA labeling and detection starter kit II (Roche Diagnostics GmbH). To monitor and normalize loading amounts of RNAs, membranes were hybridized with the random-prime DIG-labeled GAPDH (glyceraldehyde-3-phosphate dehydrogenase) probe prepared with the DIG High Prime DNA labeling and detection starter kit II (Roche Diagnostics GmbH) and visualized as described above.

RESULTS

Growth-enhancing adaptive mutations increase virion production but have no effects on the early phase of viral replication. We previously obtained adapted viruses with enhanced growth potential from long-term cultures of macaque cells infected with macaque-tropic HIV-1 5R (34) or its R5-tropic version 562 (41). While proviral clones generated from adapted viruses contained a number of mutations in scattered regions of the viral genomes, only mutations in pol-IN or env-Gp120 were found to contribute to viral growth enhancement (32). In this study, we investigated the mechanistic basis for acceleration of viral replication by the adaptive mutations in the IN-coding sequence. As indicated in Fig. 1, four mutations (N222K, F223Y, D229E, and V234I in the 3' region of the pol gene designated Pol4889-4923) were previously shown to enhance viral growth in macaque cells (32). The introduction of both N222K and V234I into human-tropic HIV-1 NL4-3 had a growth-enhancing effect in human cells similar to that observed for 5R (32). We first studied the effect of the adaptive mutations in the Pol4889-4923 region on viral replication in M8166 cells. As shown in Fig. 2A, all mutants grew more efficiently than the parental 5R virus. To examine the early replication phase, single-cycle viral infectivity was determined by infection with VSV-G-pseudotyped viruses containing a luciferase gene in the nef gene. All mutant clones exhibited infectivity similar to that of 5R (Fig. 2B). Furthermore, the four mutations did not have positive effects on viral cDNA synthesis, as measured by real-time quantitative PCR (Fig. 2C). All four growth-enhancing mutations resulted in an increase in virion production in transfected M8166 cells (Fig. 2D). An enhancement in virion production was consistently observed for pseudotyped and proviral clones in transfected 293T cells (data not shown). These results showed that the acceleration of viral replication by the adaptive mutations in the Pol4889-4923 region could be attributed to the increase in infectious virion production in producer cells.

Amino acid substitutions caused by the adaptive mutations may not be responsible for the enhancement in virion production/replication ability. All growth-enhancing mutations in the Pol4889-4923 region were nonsynonymous changes (Fig. 1). To determine whether altered amino acids were critical for the enhancement in virion production/replication efficiency, each amino acid at the four sites (N222, F223, D229, and V234) was replaced by various amino acids with different sizes and chemical properties (detailed in Table 1). The effects of amino acid substitutions at these positions on virion production and viral replica-
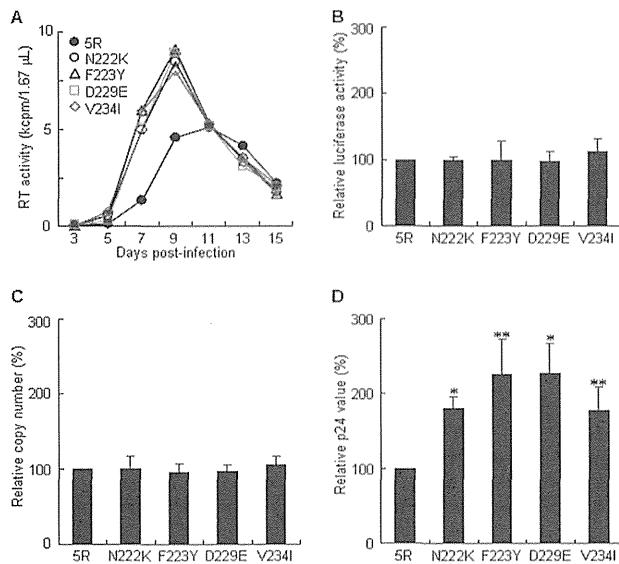
FIG 2 Effect of the adaptive mutations in the *Pol*4889-4923 region on different stages of virus replication in M8166 cells. (A) Replication kinetics. Input viruses were prepared from 293T cells transfected with the indicated proviral clones, and equal amounts were inoculated into M8166 cells. Virus replication was monitored by RT activity released into the culture supernatants. Representative data from at least three independent experiments are shown. (B) Single-cycle viral infectivity. VSV-G-pseudotyped viruses were prepared from 293T cells transfected with the indicated clones, and equal amounts were inoculated into M8166 cells. Cell lysates were prepared on day 1 postinfection and subjected to luciferase assays. Infectivity is presented as luciferase activity relative to that exhibited by 5R. Mean values from three independent experiments are shown with the standard deviations (SD). (C) Viral cDNA synthesis. VSV-G-pseudotyped viruses were prepared from 293T cells transfected with the indicated clones, DNase I treated, and inoculated into M8166 cells. Total DNA was extracted from infected cells on day 1 postinfection and subjected to real-time quantitative PCR analyses with a primer pair specific for the late form (R/gag) of viral cDNA. The DNA copy number relative to that of 5R is presented. Mean values ± SD from three independent experiments are shown. (D) Virion production. M8166 cells were cotransfected with the indicated *env*-deficient proviral clones and a luciferase reporter vector (pGL3) by using a Nucleofector. Virion production on day 2 posttransfection was measured by the amount of Gag-p24 in the culture supernatants. The amount of p24 was normalized by luciferase activity in cell lysates. The amount of p24 relative to that produced by 5R is presented. Mean values ± SD from four independent experiments are shown. Significance relative to 5R as calculated by the Student *t* test is shown (*, $P < 0.01$; **, $P < 0.02$).

tion (Fig. 3) were determined as described above. As shown in Fig. 3A, for N222, the virion production level relative to that of 5R was enhanced by the substitution with Ala (A) and Gly (G) as well as the growth-enhancing adaptive mutation Lys (K) but was decreased by the substitution with Phe (F) and Tyr (Y). The increase and decrease in virion production caused by these amino acid substitutions at N222 positively correlated with viral growth potential (Fig. 3A). For F223 (Fig. 3B), all mutant clones carrying Ala (A), Glu (E), Gly (G), His (H), Lys (K), and Ser (S) in addition to the adaptive mutation Tyr (Y) produced more virions than 5R, whereas only F223Y augmented viral replication efficiency. To study the cause of this apparent discrepancy, we compared the effects of F223Y and F223A/E/H/S on the early replication phase (Fig. 4). While F223Y showed levels of single-cycle viral infectivity and viral cDNA synthesis (late and integrated forms) similar to those for 5R, marked differences were observed in the behaviors of

the other mutants. The virus infectivity of F223H was approximately 30% to that of 5R, and the infectivity of F223A/E/S was undetectable (Fig. 4A). A reduction in viral cDNA levels was also observed for F223A/E/H/S (Fig. 4B and C). These results indicate that the F223 residue is essential for the function of IN in the early replication phase. For D229 (Fig. 3C), virion production/replication ability was enhanced only by the adaptive mutation Glu (E), and the other mutants carrying D229A/G/T/W had reduced virion production/replication potential. For V234 (Fig. 3D), the Gly (G) substitution as well as the adaptive mutation Ile (I) augmented virion production/replication capability, but V234A/W decreased these. Because mutants D229K and V234E produced virions at the 5R level upon transfection (Fig. 3C and D), they are most likely to be defective for the early replication phase like the F223 mutants (Fig. 3B and 4). The results in Fig. 3 clarify the clear correlation between virion production and viral growth potential, except for the F223 mutants and the D229K/V234E mutants. However, increases or decreases in virion production were not dependent on altered amino acid sizes or chemical properties (Table 1). For example, virion production levels were enhanced by any altered amino acids tested at F223, and V234G and V234A increased and decreased virion production levels, respectively, despite their similar amino acid properties. Therefore, these results indicate that amino acid residues may not be a determinant for virion production.

Synonymous codon changes in V234I alter virion production/replication ability. Although no clear relationship was observed between the amino acids in the *Pol*4889-4923 region and increase in virion production (Table 1), virion production levels were markedly affected by the substitutions with different amino acids (Fig. 3). Since nucleotide mutations in the IN-coding sequence can induce viral phenotypic changes as described above, we speculated about the possible involvement of codon/nucleotide sequences in virion production enhancements. Thus, proviral clones carrying different codons for growth-enhancing mutations were constructed (N222K-2, F223Y-2, D229E-2, V234I-2, and V234I-3), and their growth potentials were compared to those of 5R and parental clones with each adaptive mutation. As shown in Fig. 5A, the growth of codon-altered viral clones (N222K-2, F223Y-2, and D229E-2) was more efficient than that of 5R, as observed for N222K, F223Y, and D229E. A fluctuation in viral replication potential among the V234I codon variants was noted: the growth abilities of V234I and V234I-3 were higher than that of 5R, but that of for V234I-2 was slightly impeded (Fig. 5A). While the single-cycle early infectivities of 5R and these codon variants were similar (Fig. 5B), their virion production levels varied in parallel with their replication potentials (Fig. 5A and C). Only V234I-2 exhibited a virion production level similar to that of 5R, and the other codon-altered mutants showed an enhanced level of virion production. The results for the V234I codon variants demonstrate the alteration in virion production levels in a nucleotide sequence-dependent manner, resulting in the modulation of viral replication ability.

Virion production levels of V234I codon variants correlate with Gag and Gag-Pol expression levels in producer cells. Synonymous codon changes in Ile (I) at amino acid position 234 in *pol*-IN caused an alteration in infectious virion production levels (Fig. 5C). We assumed that at least Gag and Gag-Pol expression levels, prerequisites for virion formation, correlatively varied with the amount of progeny virions. It has also been shown that cell-

TABLE 1 Characteristics of viral clones carrying various mutations in the 3' region of the *pol* gene

Amino acid position in IN	Viral clone name	Amino acid	Codon	Size of amino acid	Chemical property(ies) of amino acid	Early replication[a]	Virion production[a]	Growth[b]
222	5R	N	AAT	Medium-small	Neutral, hydrophilic	++	++	++
	N222K[c]	K	AAA	Medium-large	Basic	++	+++	+++
	N222K-2	K	AAG	Medium-large	Basic	++	+++	+++
	N222A	A	GCT	Small	Aliphatic, hydrophobic	ND[d]	+++	+++
	N222G	G	GGT	Small	Aliphatic, hydrophobic	ND	+++	+++
	N222F	F	TTC	Large	Aromatic, hydrophobic	ND	+	−
	N222Y	Y	TAT	Large	Aromatic	ND	++	+
223	5R	F	TTT	Large	Aromatic, hydrophobic	++	++	++
	F223Y[c]	Y	TAT	Large	Aromatic	++	+++	+++
	F223Y-2	Y	TAC	Large	Aromatic	++	+++	+++
	F223H	H	CAT	Large	Basic	+	+++	+
	F223G	G	GGT	Small	Aliphatic, hydrophobic	ND	+++	−
	F223A	A	GCT	Small	Aliphatic, hydrophobic	−	+++	−
	F223S	S	TCT	Small	Neutral, hydrophilic	−	+++	−
	F223E	E	GAA	Medium-large	Acidic	−	+++	−
	F223K	K	AAA	Medium-large	Basic	ND	+++	−
229	5R	D	GAC	Medium-small	Acidic	++	++	++
	D229E[c]	E	GAA	Medium-large	Acidic	++	+++	+++
	D229E-2	E	GAG	Medium-large	Acidic	++	+++	+++
	D229K	K	AAA	Medium-large	Basic	ND	++	+
	D229A	A	GCC	Small	Aliphatic, hydrophobic	ND	+	−
	D229G	G	GGC	Small	Aliphatic, hydrophobic	ND	+	+
	D229T	T	ACC	Medium-small	Neutral, hydrophilic	ND	−	−
	D229W	W	TGG	Large	Aromatic, hydrophobic	ND	−	−
234	5R	V	GTT	Medium-small	Aliphatic, hydrophobic	++	++	++
	V234I[c]	I	ATT	Medium-small	Aliphatic, hydrophobic	++	+++	+++
	V234I-2	I	ATC	Medium-small	Aliphatic, hydrophobic	++	++	+
	V234I-3	I	ATA	Medium-small	Aliphatic, hydrophobic	++	+++	+++
	V234G	G	GGT	Small	Aliphatic, hydrophobic	ND	+++	+++
	V234A	A	GCT	Small	Aliphatic, hydrophobic	ND	+	+
	V234E	E	GAA	Medium-large	Acidic	ND	++	+
	V234W	W	TGG	Large	Aromatic, hydrophobic	ND	+	+

[a] +++, >150% of 5R activity; ++, >70 to 150% of 5R activity; +, 10 to 70% of 5R activity; −, <10% of 5R activity. Data were obtained in M8166 cells.

[b] +++, replication peaked earlier or virus production levels on the peak day were higher than those of 5R; ++, replication kinetics were similar to those of 5R; +, replication peaked later or virus production levels on the peak day were lower than those of 5R; −, replication was not detected during the observation period. Data were obtained in M8166 cells.

[c] Adaptive (growth-enhancing) mutation.

[d] ND, not done.

associated Gag was decreased for *pol*-IN deletion mutant viruses defective in virion production (20). To determine intracellular Gag and Gag-Pol expression levels, the proviral clones of 5R and V234I codon variants were transfected into 293T cells in the presence or absence of the HIV-1 protease inhibitor SQV. First, intracellular Gag-p24 and Pol-RT in the absence of SQV were measured by ELISA. While V234I and V234I-3, with improved virion production potential, expressed higher levels of Gag-p24 and Pol-RT than 5R, V234I-2 and 5R generated similar amounts (Fig. 6A). We then examined the intracellular expression patterns of Gag and Gag-Pol by Western blotting analyses. The expression profiles of Pr55^{Gag}/p24 and Pr160$^{Gag-Pol}$/p66/p51 for 5R and V234I codon variants were similar in the absence of SQV, which strongly suggested the absence of an effect of V234I mutations on viral protein processing [Fig. 6B SQV(−)]. The expression levels of Gag/Gag-Pol-related proteins were higher for V234I and V234I-3 than for 5R [Fig. 6B and C, SQV(−)]. In contrast, V234I-2 appeared to express slightly lower levels of these viral

proteins than 5R [Fig. 6B and C, SQV(−)]. This small decrease in Gag/Gag-Pol expression levels may be consistent with the similar difference observed for the viral replication kinetics of 5R and V234I-2 (Fig. 5A). The variations in Pr55^{Gag} and Pr160$^{Gag-Pol}$ expression levels in the presence of SQV appeared to be smaller than those obtained by Western blotting analyses [Fig. 6B and C, SQV(+)]. This may have been due to the weak recognition of Pr55^{Gag} and Pr160$^{Gag-Pol}$ by the antibodies used. The results described above show that the alteration in the virion production/replication potential of V234I codon variants is in parallel with the increase or decrease in Gag/Gag-Pol expression levels.

Viral replication capability can be altered by natural variations in the sequences of the 3' region of the HIV-1 *pol* gene. As observed for V234I codon variants, single-nucleotide changes resulted in alterations in virion production/replication potential through the modulation of Gag/Gag-Pol expression levels, which indicated the importance of the nucleotide sequence in the *Pol*4889-4923 region (Fig. 5 and 6). Recent studies revealed that a
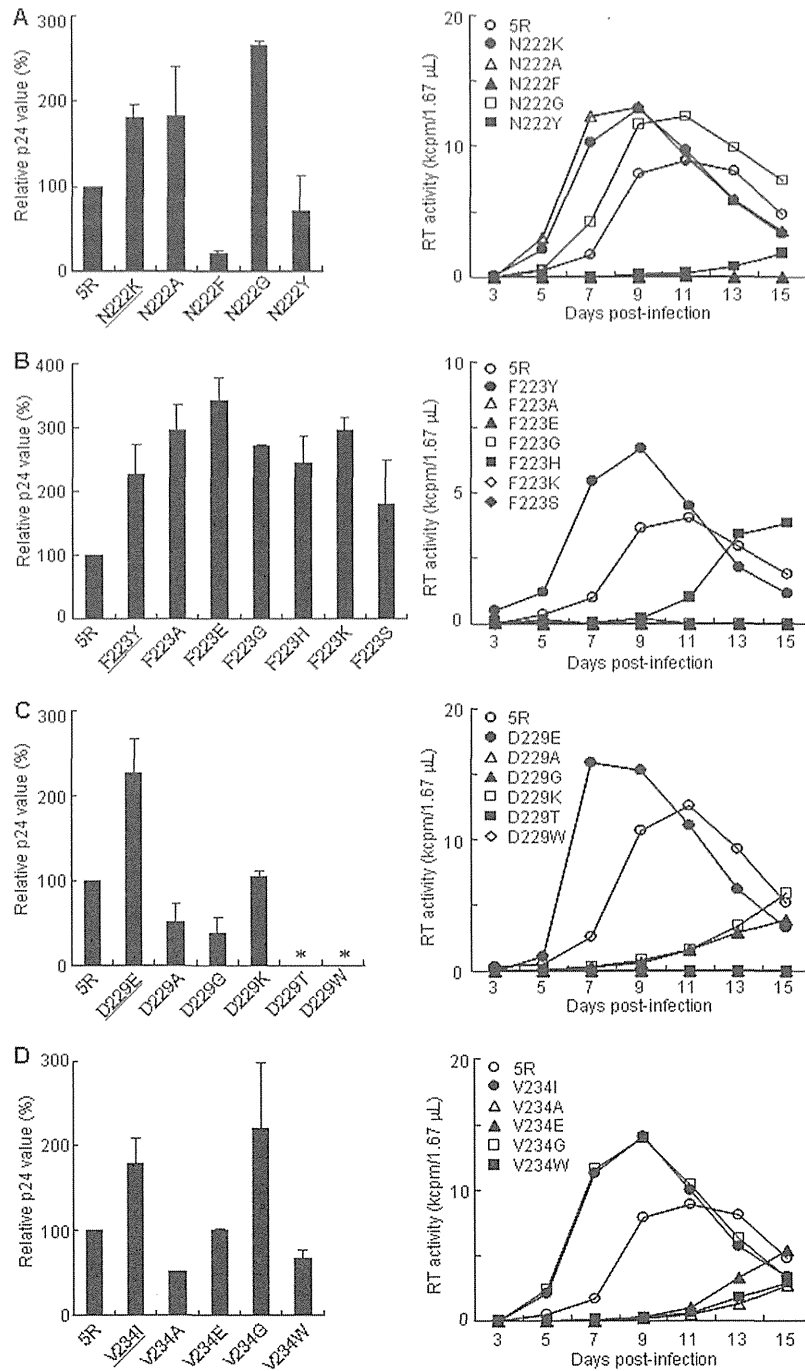
− 507 −

FIG 3 Effect of various amino acid substitutions at the N222 (A), F223 (B), D229 (C), and V234 (D) sites in the *Pol*4889-4923 region on virion production and replication kinetics. Details of the substitution for each mutant are shown in Table 1. Left panels, virion production. M8166 cells were cotransfected with the indicated *env*-deficient proviral clones and a luciferase reporter vector (pGL3) by using a Nucleofector. Virion amounts in the culture supernatants on day 2 posttransfection were measured. The amount of p24 was normalized by luciferase activity in cell lysates. The amount of p24 relative to that produced by 5R is presented. Mean values ± SD from at least two independent experiments are shown. Results for N222K, F223Y, D229E, and V234I shown in Fig. 2D (underlined) are incorporated into each panel for an easy comparison. *, under the detection limit. Right panels, viral replication kinetics. Viruses were prepared from transfected 293T cells, and equal amounts were inoculated into M8166 cells. Virus replication was monitored by RT activity released into the culture supernatants. Data in panels A and D were obtained from the same experiment, and the same result for 5R is shown separately in panels A and D as a control. Representative data from three independent experiments are shown.
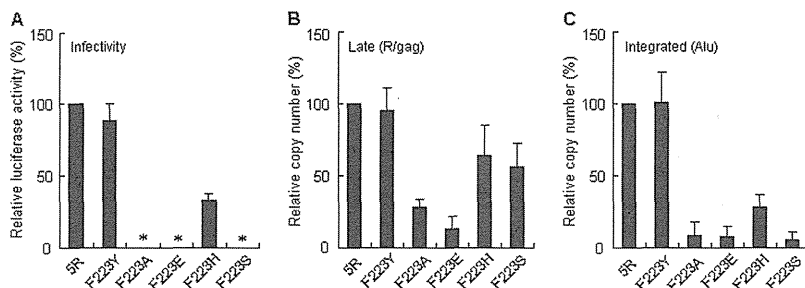
– 508 –

FIG 4 Effect of various amino acid substitutions at the F223 site on the early viral replication phases. (A) Single-cycle viral infectivity. VSV-G-pseudotyped viruses were prepared from transfected 293T cells, and equal amounts were inoculated into M8166 cells. Cells were collected and lysed on day 1 postinfection for luciferase assays. Infectivity is presented as luciferase activity relative to that exhibited by 5R. Mean values ± SD from at least four independent experiments are shown. *, mean values are <0.1%. (B and C) Monitoring viral cDNA synthesis. VSV-G-pseudotyped viruses from transfected 293T cells were treated with DNase I, and equal amounts were inoculated into M8166 cells. Total DNA was extracted from infected cells on day 1 postinfection and subjected to real-time quantitative PCR analyses with primer pairs specific for the late (B) and integrated (C) forms of viral cDNA. The DNA copy number relative to that of 5R is presented. Mean values ± SD from at least four independent experiments are shown.

naturally occurring synonymous polymorphism in some genes can influence the expression levels, structures, and functions of their encoded proteins (42–44). In addition, the IN CTD sequence is more heterogenous than those of the other IN domains (15, 17,
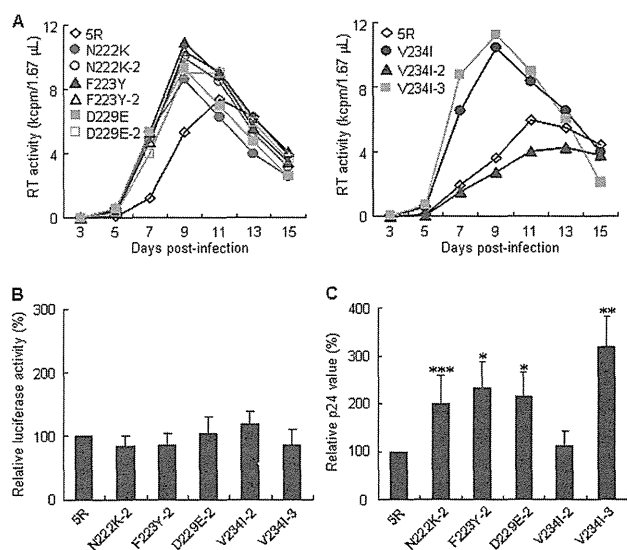

FIG 5 Effect of codon alterations at N222K, F223Y, D229E, and V234I sites on different stages of viral replication. N222K-2, F223Y-2, D229E-2, V234I-2, and V234I-3 indicate mutant clones containing an altered codon. The codon used for each mutant is shown in Table 1. (A) Viral replication kinetics. Input viruses were prepared from transfected 293T cells, and equal amounts were inoculated into M8166 cells. Virus replication was monitored by RT activity released into the culture supernatants. Representative data from at least two independent experiments are shown. (B) Single-cycle viral infectivity. VSV-G-pseudotyped viruses were prepared from transfected 293T cells, and equal amounts were inoculated into M8166 cells. Cell lysates were prepared on day 1 postinfection and subjected to luciferase assays. Infectivity is presented as luciferase activity relative to that exhibited by 5R. Mean values ± SD from at least three independent experiments are shown. (C) Virion production. M8166 cells were cotransfected with the indicated env-deficient proviral clones and a luciferase reporter vector (pGL3) by using a Nucleofector. Virion production on day 2 posttransfection was measured by the amount of p24 in the culture supernatants. The amount of p24 was normalized by luciferase activity in cell lysates. The amount of p24 relative to that produced by 5R is presented. Mean values ± SD from at least three independent experiments are shown. Significance relative to 5R as calculated by the Student t test is shown (*, P < 0.01; **, P < 0.05; ***, P < 0.1).

19). To clarify the significance of the nucleotide sequence in the Pol4889-4923 region for viral replication, we examined HIV-1 sequences within the region obtained from the HIV Sequence Compendium (Los Alamos National Laboratory, NM, USA). As shown in Table 2, while viruses carrying F223Y or D229E, which we identified as growth-enhancing mutations, were not found, those with N222K or V234I were present. We noted that codon variants with distinct growth abilities, V234I (ATT) and V234I-2 (ATC), coexisted in a viral population with different frequencies (Table 2). This suggested that there may be natural variants of HIV-1 with distinct replication potentials. Moreover, a sequence comparison in the Pol4889-4923 region revealed the presence of natural synonymous variations for parental clone 5R-encoded amino acid residues, even though the frequency was lower than that of 5R (Table 2). Thus, we examined whether viral replication can be affected by natural synonymous changes at the sites of adaptive mutations (N222, F223, D229, and V234) as well as other sites (V225, Y226, and P233) within the Pol4889-4923 region. The viral growth kinetics of 5R and its natural variants at adaptive mutation sites (N222aac, F223ttc, D229gat, and V234gtg) were determined in human MT4/CCR5 cells (Fig. 7A and Table 2). While N222aac and F223ttc exhibited growth kinetics similar or slightly better than those of 5R, the viral replication potentials of D229gat and V234gtg was markedly higher and lower, respectively, than that of 5R (Fig. 7A and Table 2). We next determined the viral growth kinetics of additional natural synonymous variants (V225gtc, Y226tac, and P233cct/ccc/ccg). Alterations in the viral replication potentials of these clones were evident: the viral replication kinetics of V225gtc were similar to those of 5R, whereas growth ability was higher for Y226tac and lower for P233cct/ccc/ccg than for 5R (Fig. 7B and Table 2). On the other hand, the genome structure of 5R is different from that of natural human-tropic HIV-1 due to the change of the cyclophilin A-binding loop-coding region in gag and of an entire vif to the corresponding regions of SIVmac239 (34). Thus, we determined whether these natural synonymous variations also affect the viral replication of human-tropic HIV-1 (NL4-3 clone). The viral growth potential of NL4-3 was altered similarly as that of 5R by natural synonymous changes: the replication abilities of D229gat and Y226tac were higher than that of NL4-3, and those of V234gtg and P233cct/ccc/ccg were lower than that of NL4-3 (Fig. 7C and D). We conclude from these results that natural variations (single-
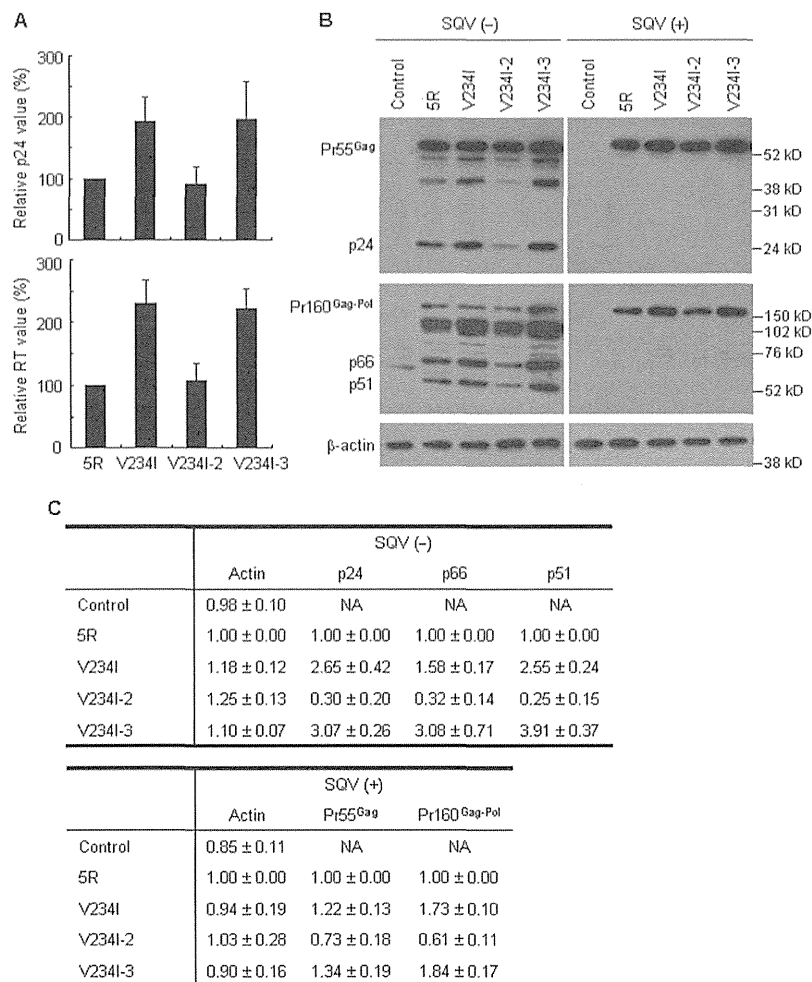
FIG 6 Effect of codon alterations at the V234I site on intracellular viral protein expression. (A) Expression levels of Gag-p24 and Pol-RT as determined by ELISA. 293T cells were transfected with the indicated proviral clones, and on day 2 posttransfection, lysates were prepared from transfected cells for the analysis of Gag-p24 and Pol-RT. The amounts of Gag-p24 and Pol-RT relative to those expressed by 5R are presented. Mean values ± SD from three independent experiments are shown. (B) Expression pattern of viral proteins as analyzed by Western blotting. 293T cells were transfected with the indicated proviral clones in the absence (−) or presence (+) of 2 μM SQV. Cell lysates were prepared from transfected cells on day 1 posttransfection, and analyzed by Western blotting using anti-p24 (upper panels), anti-RT (middle panels), and anti-β-actin (lower panels) antibodies. The migration positions of mass standards are indicated on the right. Representative data from two independent transfection experiments are shown. Control, pUC19. (C) Quantitative analysis of the Western blot. Signal intensities of viral proteins were quantitated, and the intensities relative to those with 5R proteins are shown. Mean values ± SD obtained from the two independent transfection experiments in panel B are indicated. NA, not applicable.

nucleotide synonymous mutations) in the 3′ region of the HIV-1 *pol* gene (nt 4889 to 4923 for 5R and nt 4895 to 4929 for NL4-3) can alter viral replication potential.

Natural synonymous changes influence the expression levels of intracellular viral proteins (Gag, Gag-Pol, Vpu, and Env) but not those of Nef and Rev. Gag/Gag-Pol expression levels in V234I codon variants varied correlatively with their virion production/replication abilities (Fig. 5 and 6). Env, in addition to Gag/Gag-Pol, is of course required for infectious virion formation. HIV-1-encoded proteins are translated from distinct viral mRNA species, and the regulation of gene expression is different for early transcripts (completely spliced form) and late transcripts (singly spliced and unspliced forms). To investigate further the virological effect of single-nucleotide natural variations, we determined the expression levels of products from various mRNA species: Gag

and Gag-Pol from the unspliced form, Vpu and Env from the singly spliced form, and Nef and Rev from the completely spliced form. Proviral clones (5R, Y226tac, D229gat, P233ccc, V234I, and V234gtg) were transfected into 293T cells, and cell lysates prepared on day 1 posttransfection were analyzed by Western blotting. Although V234I was not a synonymous change in the *Pol*4889-4923 region, this clone was included in this analysis because V234I is a single-nucleotide natural variant of V234 in 5R, and its virion production/replication ability was increased or decreased by single-nucleotide substitutions at this position (Table 2). As shown in Fig. 8A, we confirmed that virion production levels in transfected 293T cells correlated with viral replication potential (Fig. 2, 7, and 8A) (upregulated, Y226tac, D229gat, and V234I; downregulated, P233ccc and V234gtg). We then examined the intracellular expression level of each viral protein (Fig. 8B).

TABLE 2 Amino acid/codon frequency in the 3' region of the *pol* gene (nt 4889 to 4923 for 5R and nt 4895 to 4929 for NL4-3) of HIV-1/SIVcpz[a]

Amino acid position in IN	Amino acid frequency[b]			Codon frequency[b]			Growth[c]
	Amino acid	No.	%	Codon	No.	%	
222	N[d]	179	91.3	AAT[d]	175	89.3	+ +
				AAC	4	2.0	+ +/+ + +
	K[e]	14	7.1	AAA[e]	14	7.1	+ + +
	Q	2	1.0	CAA	2	1.0	ND[f]
	D	1	0.5	GAT	1	0.5	ND
223	F[d]	196	100.0	TTT[d]	183	93.4	+ +
				TTC	13	6.6	+ +/+ + +
	Y[e]	0	0.0	TAT[e]	0	0.0	+ + +
225	V[d]	195	99.5	GTT[d]	175	89.3	+ +
				GTC	20	10.2	+ +
	L	1	0.5	CTT	1	0.5	ND
226	Y[d]	194	99.0	TAT[d]	193	98.5	+ +
				TAC	1	0.5	+ + +
	F	1	0.5	TTT	1	0.5	ND
	H	1	0.5	CAT	1	0.5	ND
229	D[d]	196	100.0	GAC[d]	194	99.0	+ +
				GAT	2	1.0	+ + +
	E[e]	0	0.0	GAA[e]	0	0.0	+ + +
233	P[d]	194	99.0	CCA[d]	135	68.9	+ +
				CCT	35	17.9	+
				CCC	23	11.7	+
				CCG	1	0.5	+
	S	1	0.5	TCA	1	0.5	ND
	T	1	0.5	ACC	1	0.5	ND
234	V[d]	26	13.3	GTT[d]	25	12.8	+ +
				GTG	1	0.5	+
	I[e]	128	65.3	ATT[e]	127	64.8	+ + +
				ATC	1	0.5	+
	L	40	20.4	CTT	39	19.9	ND
				CTG	1	0.5	ND
	S	1	0.5	AGC	1	0.5	ND
	T	1	0.5	ACT	1	0.5	ND

[a] For 196 sequences of HIV-1/SIVcpz complete genomes from the HIV Sequence Compendium, 2011 (Los Alamos National Laboratory; http://www.hiv.lanl.gov).
[b] Relative to 196 sequences of HIV-1/SIVcpz strains.
[c] + + +, replication peaked earlier or virus production levels on the peak day were higher than those of the parental clones; + +, replication kinetics were similar to those of the parental clones; +, replication peaked later or virus production levels on the peak day were lower than those of the parental clones. Data were obtained in M8166 or MT4/CCR5 cells.
[d] Amino acid encoded or codon usage in parental clones.
[e] Amino acid encoded or codon usage in adapted (growth-enhanced) viruses.
[f] ND, not done.

The intracellular expression levels of Gag, Gag-Pol, Vpu, and Env varied among the clones tested and correlated with viral replication potential: clones with enhanced growth efficiencies expressed higher levels of these proteins, and vice versa (Fig. 2, 7, and 8B and C). In contrast, the expression levels of Nef and Rev by all proviral clones tested were similar to that of 5R, and they were constant for all variants with different virion production/replication potentials (Fig. 2, 7, and 8). Furthermore, Tat activity was determined by cotransfection assays with 5R, its single-nucleotide variants, and the 5RLTR-Luc reporter construct. No significant difference in the abilities of these proviral clones to *trans*-activate luciferase gene expression was observed, which indicated that 5R and its variants had similar Tat activity (Fig. 8D). These results suggest

that single-nucleotide changes in the *Pol*4889-4923 region can alter virion production/replication potential by modulating the expression levels of late (but not early) viral proteins.

Naturally occurring single-nucleotide variations change the expression patterns of HIV-1 mRNA species. Naturally occurring single-nucleotide mutations that alter the expression levels of viral late proteins were Y226tac, D229gat, V234I, P233ccc, and V234gtg (Fig. 8). We noted that these mutations clustered in the region proximal to the splice acceptor A1 (SA1) site (designated SA1prox in Fig. 9A). To determine the mechanistic basis for the altered phenotype, we analyzed the effect of single-nucleotide changes on the profiles of viral mRNA expression. 293T cells were transfected with parental clones (5R and NL4-3) or their mutants,
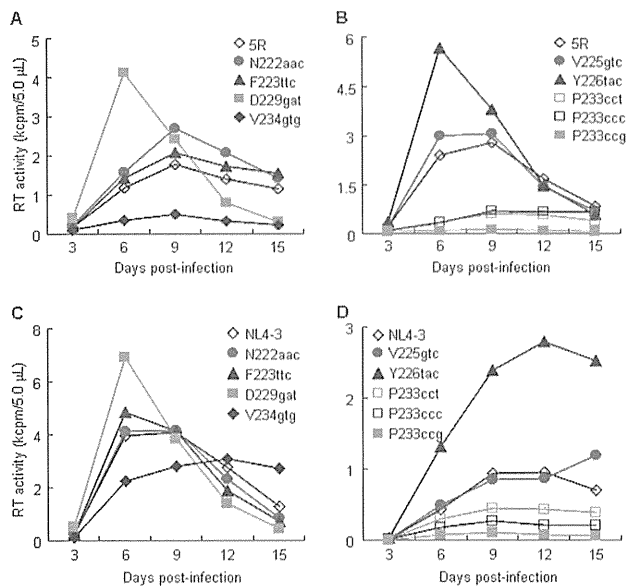
FIG 7 Effect of single-nucleotide synonymous changes in the *Pol*4889-4923 region on viral replication potential. Viruses were prepared from transfected 293T cells, and equal amounts were inoculated into MT4/CCR5 cells. Virus replication was monitored by RT activity released into the culture supernatants. Representative data from two independent experiments are shown.

and DNase I-treated poly(A)$^+$ RNAs were prepared from total cell RNAs at 10 to 20 h posttransfection. Northern blot analysis of these samples using a probe (U probe) to detect all HIV-1 mRNA species (Fig. 9B) was then performed (Fig. 9C). Because no significant difference in the RNA expression patterns for the samples of each clone prepared at 10 and 20 h posttransfection was noted (data not shown), we comparatively analyzed viral mRNAs in cells at the latter time point. As shown in Fig. 9C, the expression levels of viral late proteins did not directly correlate with the steady-state levels of their respective transcripts (9 kb and 4 kb) (Fig. 8B and 9C, left panel). The total amounts of viral mRNAs, especially the 1.8-kb mRNA species, were lower for the clones with increased viral late protein expression (Y226tac, D229gat, and V234I) than for 5R and the other mutants (P233ccc and V234gtg). However, single-nucleotide mutations always gave unique viral mRNA expression profiles. Several bands (*1 to *4 in Fig. 9C, left panel) other than the three major viral RNA species (1.8 kb, 4 kb, and 9 kb) were more or equally intense for P233ccc and V234gtg, with the poor expression of late proteins, and less intense for Y226tac, D229gat, and V234I, with the high expression of late proteins, than for 5R. Similar results, albeit to a lesser extent, were obtained for NL4-3 and its mutants with higher or lower abilities to replicate in cells (Fig. 9C, right panel). As such, viruses with a relatively high replication ability in each group (5R and NL4-3) appeared to be tuned up to have three major mRNA species. Northern blot analysis using HeLa cells was performed to exclude the possibility that the viral mRNA expression pattern described above was 293T cell specific. Results similar to those in 293T cells were obtained for 5R, NL4-3, and their mutants (D229gat and V234gtg) (data not shown). Taken together, our results here show that single-nucleotide changes in the SA1prox affect the expression patterns of viral mRNA species and suggest that this transition may lead to

the enhancement or reduction in viral late protein expression/replication efficiency.

To identify the nature of transcripts detected as extra bands (*1 to *4) (Fig. 9C), we performed Northern blot analysis using RRE, vif, and vpr probes (Fig. 9B). As expected, 9-kb transcripts but not 1.8-kb transcripts were detected by the RRE, vif, and vpr probes (Fig. 9D). While all transcripts longer than 4 kb were detected by the RRE probe, the vif and vpr probes recognized the species *1 to *3 and *1 to *4, respectively. The *2 band was more intense with the vpr probe than with the vif probe. Thus, the *1 species contained the *vif* transcript (Fig. 9B), and the *2 band consisted mainly of the *vpr* transcript (Fig. 9B). Transcripts *3 and *4 contained the Vif/Vpr-coding region and Vpr-coding region, respectively, without the RRE region.

Northern blot analysis revealed that the lower expression of late proteins by 5R, P233ccc, and V234gtg was linked to the abundance of transcripts, especially the *1 and *3 species. We hypothesized that these abundant transcripts may disturb the expression of late proteins. To test this possibility, we performed interference assays by the cotransfection of D229gat and 5R/V234gtg (Fig. 10). If the extra transcripts *1 and *3 interfere with translation from transcripts corresponding to late proteins, the Gag-p24 expression levels of D229gat would be proportionally decreased upon cotransfection with increasing amounts of 5R or V234gtg. As shown in Fig. 10 (top and middle panels), p24 expression levels were increased in cells upon single transfection of D229gat, 5R, or V234gtg with an increasing DNA amount, and marked differences were observed between each clone (D229gat > 5R > V234gtg). When a constant amount of D229gat and an increasing amount of 5R or V234gtg were cotransfected, p24 expression levels reflected just the addition of the amount produced by each clone. Virion production from cells correlated well with the intracellular p24 expression levels (data not shown). Cotransfection assays using D229gat and the *gag/gag-pol* frameshift mutant of V234gtg (gtg-Spe), which is incapable of producing p24, were performed to confirm this result. As is clearly observed in Fig. 10 (bottom panel), the increase in the amount of the gtg-Spe clone did not affect p24 expression levels produced from D229gat. Taken together, these results suggest that a large amount of transcripts (especially the *1 and *3 species) in 5R and V234gtg clones does not interfere with Gag-p24 expression and also that the single-nucleotide changes in the SA1prox act on the expression of late proteins in *cis*.

DISCUSSION

In this study, we demonstrated that four adaptive mutations in the 3′ region of the *pol* gene encoding IN upregulated the viral replication potential by increasing virion production levels without any effects on the early replication phase (Fig. 2). Moreover, the identification of V234I codon variants that have different abilities to produce virions and replicate in cells suggested regulation by single-nucleotide changes (Fig. 5). A comparative investigation of nucleotide sequences in the 3′ region of the *pol* gene (nt 4889 to 4923 for 5R and nt 4895 to 4929 for NL4-3) has revealed that these variants naturally coexist in a viral population (Table 2). We show here that naturally occurring synonymous changes (Y226tac, D229gat, P233cct/ccc/ccg, and V234gtg) can alter the viral replication potentials of HIV-1 5R and NL4-3 (Fig. 7 and Table 2).

The naturally occurring single-nucleotide variations that alter viral replication potential clustered in the SA1prox (Fig. 9A).
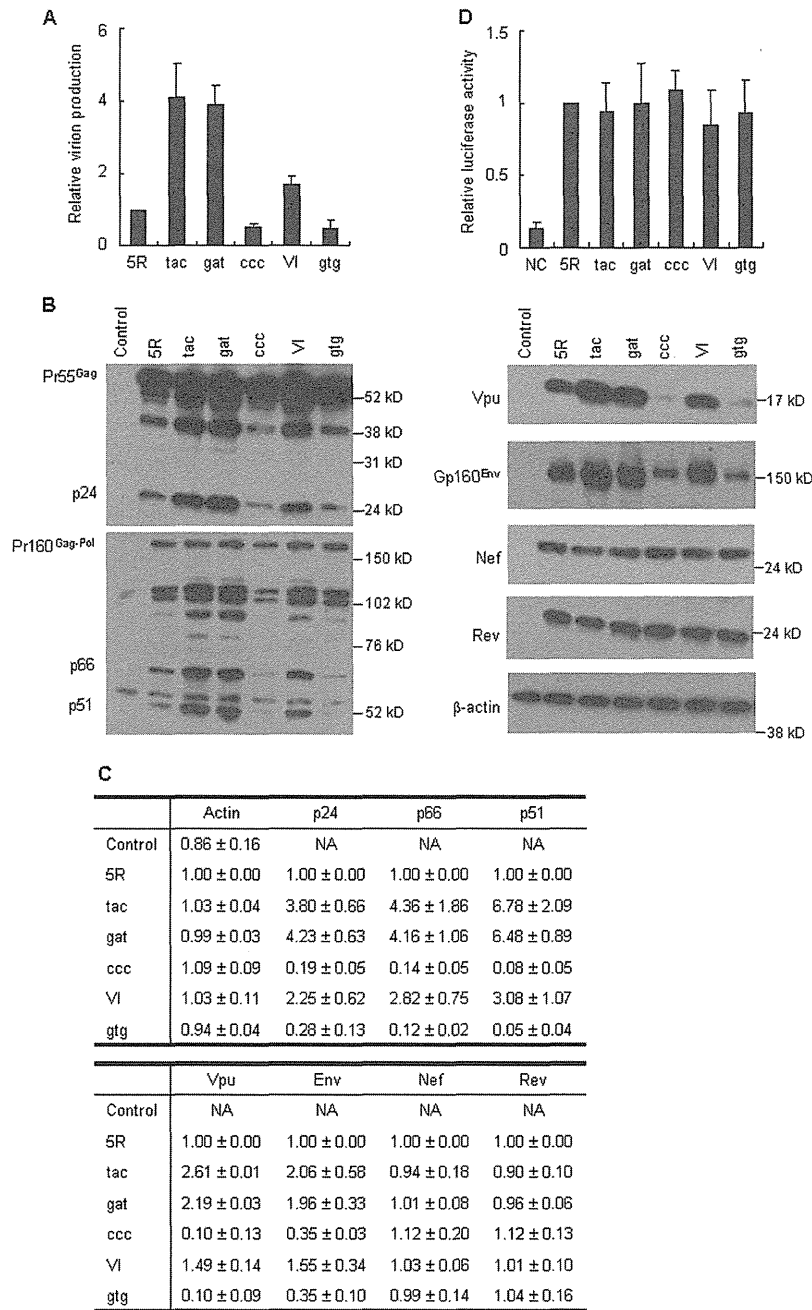
– 512 –

A — Relative virion production; bars for 5R, tac, gat, ccc, VI, gtg

D — Relative luciferase activity; bars for NC, 5R, tac, gat, ccc, VI, gtg

B — Western blots

Left panel (Control, 5R, tac, gat, ccc, VI, gtg):
- Pr55^Gag — 52 kD, 38 kD, 31 kD
- p24 — 24 kD
- Pr160^Gag-Pol — 150 kD, 102 kD, 78 kD
- p66, p51 — 52 kD

Right panel (Control, 5R, tac, gat, ccc, VI, gtg):
- Vpu — 17 kD
- Gp160^Env — 150 kD
- Nef — 24 kD
- Rev — 24 kD
- β-actin — 38 kD

C

	Actin	p24	p66	p51
Control	0.86 ± 0.16	NA	NA	NA
5R	1.00 ± 0.00	1.00 ± 0.00	1.00 ± 0.00	1.00 ± 0.00
tac	1.03 ± 0.04	3.80 ± 0.66	4.36 ± 1.86	6.78 ± 2.09
gat	0.99 ± 0.03	4.23 ± 0.63	4.16 ± 1.06	6.48 ± 0.89
ccc	1.09 ± 0.09	0.19 ± 0.05	0.14 ± 0.05	0.08 ± 0.05
VI	1.03 ± 0.11	2.25 ± 0.62	2.82 ± 0.75	3.08 ± 1.07
gtg	0.94 ± 0.04	0.28 ± 0.13	0.12 ± 0.02	0.05 ± 0.04

	Vpu	Env	Nef	Rev
Control	NA	NA	NA	NA
5R	1.00 ± 0.00	1.00 ± 0.00	1.00 ± 0.00	1.00 ± 0.00
tac	2.61 ± 0.01	2.06 ± 0.58	0.94 ± 0.18	0.90 ± 0.10
gat	2.19 ± 0.03	1.96 ± 0.33	1.01 ± 0.08	0.96 ± 0.06
ccc	0.10 ± 0.13	0.35 ± 0.03	1.12 ± 0.20	1.12 ± 0.13
VI	1.49 ± 0.14	1.55 ± 0.34	1.03 ± 0.06	1.01 ± 0.10
gtg	0.10 ± 0.09	0.35 ± 0.10	0.99 ± 0.14	1.04 ± 0.16

FIG 8 Effect of single-nucleotide changes on virion production and intracellular expression levels of viral proteins. (A) Virion production in transfected cells. 293T cells were transfected with the indicated proviral clones, and on day 1 posttransfection, virion production was monitored by the amount of Gag-p24 in the culture supernatants. The amount of p24 relative to that produced by 5R is presented. Mean values ± SD from three independent experiments are shown. (B) Expression of various viral proteins in transfected cells. 293T cells were transfected with the indicated proviral clones, and on day 1 posttransfection, cell lysates were prepared for Western blotting using anti-Gag-p24, anti-RT, anti-Vpu, anti-Env-gp160, anti-Nef, anti-Rev, and anti-β-actin antibodies. The migration positions of mass standards are indicated on the right. Representative data from two independent transfection experiments are shown. Control, pUC19; tac, Y226tac; gat, D229gat; ccc, P233ccc; VI, V234I; gtg, V234gtg. (C) Quantitative analysis of the Western blot. Signal intensities of viral proteins were quantitated, and the intensities relative to those for 5R proteins are shown. Mean values ± SD obtained from the two independent transfection experiments in panel B are indicated. NA, not applicable. (D) Analysis of Tat activity. 293T cells were cotransfected with the indicated proviral clones and an LTR-driven luciferase reporter clone, and on day 1 posttransfection, cell lysates were prepared for luciferase assays. Luciferase activity relative to that exhibited by 5R is presented. Mean values ± SD from three independent experiments are shown. NC, negative control (basal luciferase activity of the LTR-driven luciferase reporter clone in the absence of proviral clones).
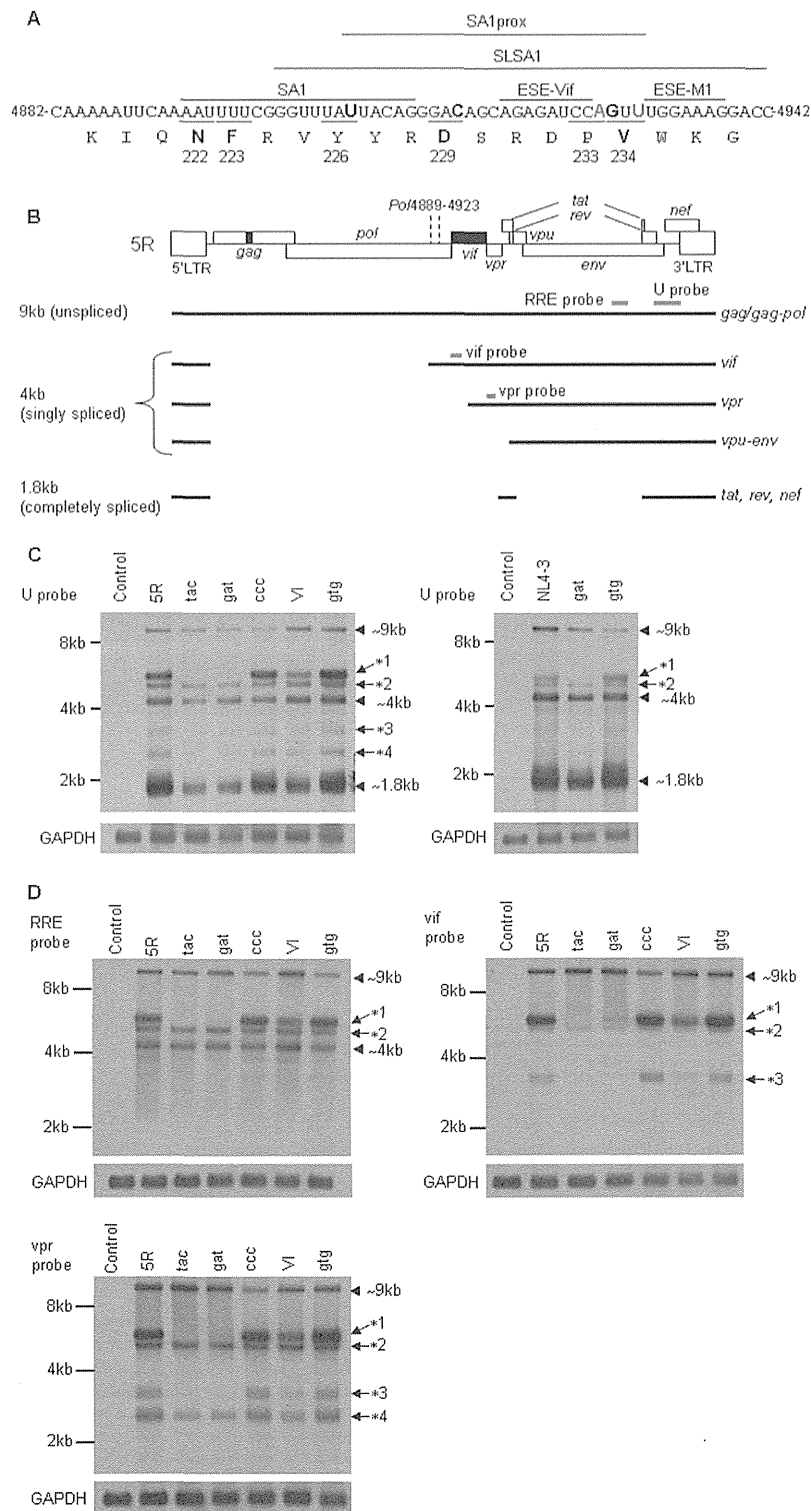
– 513 –

FIG 9 Effect of single-nucleotide changes on viral mRNA expression. (A) Nucleotide and amino acid sequences in the 3' region of the *pol* gene. Nucleotides 4882 to 4942 correspond to the NL4-3 sequence (35) (GenBank accession no. AF324493). Black and gray bold letters in the nucleotide sequence show the sites at which the single-nucleotide substitution promoted or decreased viral replication efficiency, respectively. Bold letters in the amino acid sequence represent adaptive mutation sites. The SA1prox (this study), SA1 site (3, 4), ESE-Vif (27), ESE-M1 (28), and SLSA1 region (45) are as indicated. Numbers and underlines show the positions of amino acids in IN and their codons, respectively. (B) Schematic presentation of the 5R genome organization and various HIV-1 mRNA species. The genome structure of 5R is shown as in Fig. 1. Gray bars represent the regions used as probes for Northern blot analyses. The *Pol*4889-4923 region is also indicated.
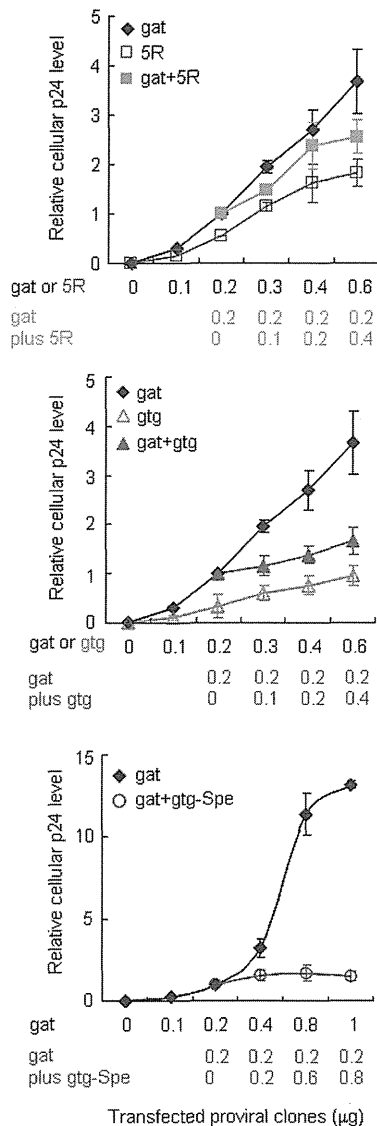
FIG 10 Expression level of Gag-p24 in singly or doubly transfected cells. 293T cells were transfected with proviral clones as indicated, and on day 1 posttransfection, Gag-p24 expression level in cell lysates was determined. The amount of p24 relative to that produced upon transfection with 0.2 μg of the D229gat (gat) clone is presented. Mean values ± SD from three independent experiments are shown. gat, D229gat; gtg, V234gtg; gtg-Spe, a frameshift mutant of V234gtg.

These mutations were identified by both viral adaptation experiments (32) and comparative analysis of numerous HIV-1/SIVcpz genomes (Table 2). These findings suggest that the nucleotide sequence in the SA1prox may be involved in the viral adaptation/

evolution process. Recent RNA structure analysis has shown that the nucleotide sequence proximal to SA1 within the HIV-1 genome forms a stem-loop structure (45, 46). Moreover, Pollom et al. reported that this stem-loop structure, designated "SLSA1," was conserved between HIV-1 NL4-3 and SIVmac239, suggesting the virological importance of the SLSA1 structure (45). Interestingly, all single-nucleotide mutations analyzed in Fig. 8 and 9 were mapped onto the SLSA1 sequence (at positions 4901 to 4942 in Fig. 9A). The emergence of novel mutations within this region may be limited due to its effect on IN functions, SA1 functions, and the SLSA1 structure. This may explain the low frequency of single-nucleotide mutations that alter viral replication efficiencies among HIV-1 genomes (Table 2). Nevertheless, the presence of such single-nucleotide variations in SLSA1 represents the plasticity of viruses with the ability to adapt themselves under various constraints. Our results on the replication-altering mutations within SLSA1 may also be useful for analyzing changes in the RNA sequence/structure and their effects on viral replication. Because the SLSA1 structure is conserved between HIV-1 NL4-3 and SIVmac239, it is of interest to determine whether naturally occurring single-nucleotide synonymous mutations in this region affect the replication efficiency of SIVmac239 and its closely related primate lentiviruses.

The change in virion production/replication ability was reflected in the expression levels of viral late proteins (Gag, Gag-Pol, Vpu, and Env) but not in those of the early proteins (Nef and Rev) (Fig. 7 and 8). However, a direct positive correlation between the steady-state levels of viral mRNAs and their corresponding late proteins was not observed (Fig. 8 and 9). More viral RNAs and a large number of viral RNA species were synthesized in cells producing low expressors of viral late proteins (5R, P233ccc, and V234gtg) than in those producing high expressors (Y226tac, D229gat, and V234I). This may imply that the expression level of mRNAs directed by high expressors is necessary and sufficient for the efficient expression of viral proteins and optimal viral replication. We initially assumed that various kinds of viral transcripts by low expressors may hinder the efficient translation of viral late proteins. However, interference assays between variants (Fig. 10) showed that this prediction may not be accurate. Moreover, no significant difference in the Tat activity of 5R and its variants was observed (Fig. 8D). Therefore, it is reasonable to assume that single-nucleotide changes in the SA1prox act in *cis* and may influence splicing, mRNA stability, mRNA transport, and/or translation efficiency from mRNAs.

The abundance of the *vif* transcript (species *1 in Fig. 9C and D) observed for 5R and low expressors (P233ccc and V234gtg) suggests enhanced splicing at the SA1 site. On one hand, a combination of two synonymous mutations in SLSA1 that changes its RNA structure was reported to affect splicing at the SA3 site downstream of SA1 but not that at the SA1 site, showing long-range RNA interactions and cross talk between splicing sites (45). This may explain variations in the expression levels of transcripts (the

RRE, Rev-responsive element; U, universal. (C and D) Steady-state expression levels of HIV-1 mRNA species. Total RNA was prepared from 293T cells transfected with the indicated proviral clones, and poly(A)$^+$ RNA was selected. After the DNase I treatment, samples were subjected to Northern blot analysis using the indicated probe. GAPDH was used as an internal standard. Three major species of viral mRNA (~9 kb, ~4 kb, and ~1.8 kb) are shown by arrowheads. The other extra bands *1 to *4 are indicated by arrows. RNA size markers (8 kb, 4 kb, and 2 kb) are on the left. Representative data from four independent experiments (C, left panel [5R and its mutants]) and from two independent experiments (C, right panel [NL4-3 and its mutants] and D) are shown. Control, pUC19; tac, Y226tac; gat, D229gat; ccc, P233ccc; VI, V234I; gtg, V234gtg.